GEO 511: Master‘s Thesis

Submission Date: September 29th 2014

A Feasibility Study Modelling Hydrological Cycles using Tree-Ring Based Climate Reconstructions

Eric Gasser [09-730-581]

Supervisors:

Dr. Paolo Cherubini,

Swiss Federal Research Institute WSL, Zuercherstrasse 111, CH-8903 Birmensdorf, paolo.cherubini@wsl.ch;

Dr. Massimiliano Zappa,

Swiss Federal Research Institute WSL, Zuercherstrasse 111, CH-8903 Birmensdorf, massimiliano.zappa@wsl.ch;

PD Dr. Ulf Buentgen,

Swiss Federal Research Institute WSL, Zuercherstrasse 111, CH-8903 Birmensdorf, ulf.buentgen@wsl.ch.

Faculty Member:

Prof. Dr. Markus Egli

Abstract

Global climate change is occurring and has been recorded by numerous physical and biogeochemical observations and paleoclimatic proxy records. More and more the importance of providing a comprehensive view on Earth system processes including the hydrosphere is emerging as the ecological importance and the human vulnerability on water resource management is increasing. Hydrological observations may go as far as centuries at best, so it is an ongoing challenge to extend the hydrological record beyond instrumental observations. Providing a comprehensive view on hydrological processes over a long time-scale can support future climate predictions and would allow a more detailed analysis on climate interactions. One possibility to extend the hydrological record is by using proxy records. However, proxy records that allocate events to an exact year (i.e. tree-rings) only permit seasonal reconstructions. Modelling hydrological cycles can compute total runoff every hour or even every minute, but usually require either time-consuming calibration procedures, physical information that is simply missing, or both.

As a first attempt, we implemented seasonal precipitation and temperature reconstructions based on tree-ring chronologies into the hydrological modelling system PREVAH (PREcipitation-Runoff-EVapotranspiration HRU model) to model past annual and monthly hydrological cycles back to 500 B.C. Two Swiss catchments were selected for which the hydrological modelling System PREVAH has been successfully calibrated: The Murg stream in the canton of Thurgau and the Dischmabach stream in the canton of Graubuenden. Unfortunately, due to an internal model error, false volume corrections were computed by PREVAH. Therefore, no statistical tests regarding absolute values were conducted. However, correlation coefficients *r* outside the models calibration period were as high as 0.37 for monthly runoff simulations whereas monthly runoff simulations within the models calibration period were as high as 0.94. Obviously, the results outside the models calibration period are not statistically significant, but if the models error can be identified and fixed, proper model evaluation statistics could be conducted. As for now, the model does however detect paleohydrological trends but the results are strongly dependent on the quality of the tree-ring series.

Table of Contents

List of Figures

List of Tables

1. Introduction

1.1 Introduction

Physical and biogeochemical observations have proven continuous global climate change. Paleoclimatic proxy records extend the climate record hundreds to millions of years, providing a comprehensive view on long-term changes in the atmosphere, the ocean, the cryosphere and the land surface (IPCC 2013). The hydrological cycle is of great importance in Earth system processes as well as in socioeconomics. The ecological importance and the human vulnerability on water recourses is increasing rapidly, yet the temporal extend of hydrological records are short and may not provide essential information on the natural variability of hydrological phenomena (Salas et al. 2014). Providing knowledge of the hydrological cycle outside the instrumental records is referred to as historical hydrology or paleohydrology, aiming to extend the instrumental record for better future hydrological predictions (Brázdil & Kundzewicz 2006). One opportunity to extend the hydrological record is by modelling; the challenge is however to circumvent the gap of missing information.

Hydrological and climatological model performances have significantly improved in recent decades, also due to the enhancement of computational power. Modelling the hydrological cycle at regional and global scales is important to have a better understanding on physical, chemical and biological processes linked to natural hazards, extremes, hydropower and water resource management (Viviroli et al. 2009). A model however will always be a simplification of reality and the complex interactions involved in hydrological processes will never be fully operational (Davie 2008). One of numerous hydrological models in use is the semi-distributed conceptual modelling system PREVAH (PREcipitation-Runoff-EVApotranspiration-HRU model) which was originally developed to understand hydrological processes in mountainous catchments (Viviroli et al. 2009). Therefore, precipitation and temperature anomalies, obtained by tree-ring chronologies from the Greater Alpine Region, were implemented into PREVAH as an attempt to model past annual and monthly hydrological cycles for two Swiss catchments: The Murg stream in the canton of Thurgau and the Dischmabach stream in the canton of Graubuenden. This idealistic approach should be considered a feasibility study.

Already in the mid 1970's it was acknowledged that paleoclimatic research offers an approach to better estimate past climatic variability and it can help to design more robust water-resource systems (Fritts 1976; LaMarche 1978). The lack of instrumental runoff information was recognized at an early stage, and subsequent attempts to reconstruct streamflow events based on tree-ring chronologies commenced rapidly. While Wallis and O'Connell (1973) for instance questioned the reliability of historic hydrological records, Holmes et al.'s (1979) answer to that matter was a correlation between tree-ring and total yearly runoff in Argentina extending back to the year 1601. Cook and Jacoby (1983) presented a 248 year long streamflow reconstruction to discuss drought frequencies in the United States of America to offer a more robust water-resource system to estimate drought probabilities. Cook and Jacoby (1983) however emphasize that the results are obviously related to the quality of the tree-ring records, but generally conclude to have coped runoff reconstruction with tree-ring series. Brito-Castillo et al. (2003) applied multivariate statistical techniques to reconstruct winter streamflow from tree-ring series and debated that streamflow reconstructions are attainable on a decadal time scale. Akkemik et al. (2008) achieved statistically significant results in Turkey comparing tree-ring data with instrumental observations and historical documents. Salas et al. (2014) realized that tree-ring chronologies continuously underestimated the variability of the streamflows and attempted to model past droughts with tree-ring series adding noise to the tree-ring data.

So, reconstructing past runoff events based on tree-ring records have been attempted numerous times, but for the first time an actual semi-distributed conceptual model is used. The tree-ring data, with regional precipitation and temperature reconstructions, were provided by Dr. Ulf Buentgen who amongst others compiled tree-ring chronologies extending back to the year (a) 500 B.C. and (b) 760 A.D. Two tree-ring datasets, each from different locations within the Greater Alpine Region, were implemented into the existing hydrological modelling System PREVAH as substitution for precipitation and temperature measurements. Due to the fact that the tree-ring series were compiled from spatially scattered locations, the deviations from a long-term estimate, also known as anomalies or the delta approach (Hay et al. 2000), were used. In order for PREVAH to compute entire hydrological cycles, other climate data are needed such as sunshine duration, cloud cover, relative humidity and wind speed. To circumvent this gap of missing information the models calibrated

pre-settings were distributed randomly to fit the temporal extend of both tree-ring series. Unfortunately, this procedure automatically induces uncertainties, but it was the only way to reflect a natural variability and to replace the missing information. Model evaluation statistics would have been performed as suggested by Moriasi et al. (2007), but all of the test statistics regarding absolute values were false and unusable because of an internal model error. This unfortunate fact prevents any accurate statement on the attempt to model past hydrological cycles thus the volumes were not computed the way they should have been. In order to repeat our attempt, the cause of the models error needs to be identified and fixed. Nevertheless, correlation coefficients were calculated to properly evaluate this first attempt.

1.2 Research Questions

Specific research questions were proposed:

(a) Can dendrochronology successfully reconstruct annually resolved precipitation and temperature anomalies?
(b) What are spatial and temporal limitations in dendrochronology reconstructing climate anomalies?
(c) Can tree-ring chronologies extend the hydrological record using the hydrological modelling system PREVAH?

2. Materials & Methods

2.1 Tree-Ring Data

2.1.1 Sample Sites

Tree-ring chronology measurements were digitally provided by Dr. Ulf Buentgen. The tree-ring series with precipitation and temperature anomalies were compiled from numerous geographical locations covering the Greater Alpine Region, thus millennium-long tree-ring based precipitation and temperature reconstructions exist spatially scattered in northern Scandinavia and the Alps (Buentgen & Tegel 2011):

(a) The Swiss Alps, namely the Loetschental in the canton of Valais,
(b) The Austrian Alps, namely the Oetztal in the federal state of Tirol,
(c) Northeastern France and
(d) North- and southeastern Germany.

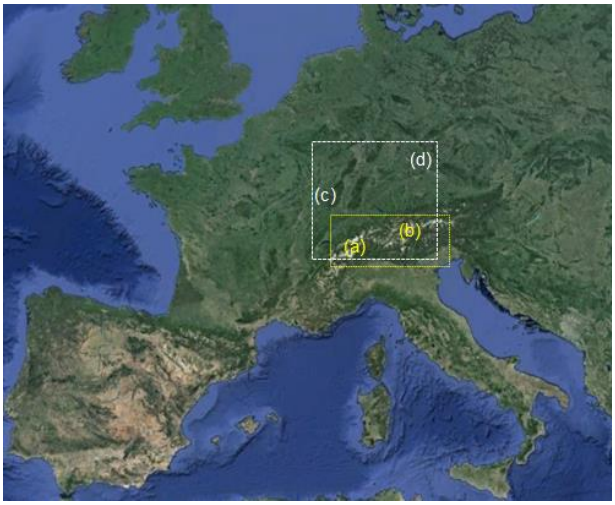

Figure 1: Satellite image over Europe.

In yellow: Location of the temperature sensitive European larch and stone pine samples. In white: Location of the precipitation sensitive European oak samples. All letters correspond to the approximate locations of the sampled trees. Source: Google Earth ©

The Greater Alpine Region consists of the European Alps and its wider surroundings (Switzerland, Liechtenstein, Austria, Slovenia, Croatia and parts of France, Germany, Italy, Czech Republic, Slovakia, Hungary, Bosnia and Herzegovina) comprising high climatic variability within its surface of approximately 714'000 km^2 (Auer et al. 2007).

Anomalies, also referred to as the delta approach (Hay et al. 2000), are deviations of an estimated climate signal (e.g. temperature or

precipitation) from a long term observed mean value, adding the difference (delta) to an observational database to transfer climate change signals into a (hydrological) model (Andréasson et al. 2004; Graham et al. 2007).

2.1.2 Precipitation

April-June-July (AJJ) precipitation anomalies were reconstructed based on 7284 precipitation-sensitive oak (*Quercus* L.) tree-ring width series from subfossil, archeological, historical and recent material sampled in northeastern France as well as in north- and southeastern Germany (Buentgen et al. 2011). The annually resolved temporal resolution covers nearly 2500 years ranging from 398 B.C. to 2008 A.D.

2.1.3 Temperature

Two temperature tree-ring series were provided:

(a) June-July-August (JJA) temperature anomalies were reconstructed based on 1089 stone pine (*Pinus cembra* L.) and 457 European larch (*Larix decidua* Mill.) tree-ring width series from high-elevation sites in the Austrian Alps, namely from the Oetztal (Buentgen et al. 2011). The annually resolved temporal resolution covers 2500 years ranging from 499 B.C. to 2003 A.D.

(b) June-July-August-September (JJAS) temperature anomalies were reconstructed based on 180 European larch tree-ring latewood density series from near timberline sites, subalpine construction timbers and historical buildings from the Swiss Alps, namely the Loetschental in the canton of Valais (Buentgen et al. 2006). The annually resolved temporal resolution covers nearly 1250 years ranging from 755 A.D. to 2004 A.D.

The precipitation and the temperature reconstructions were compiled into two tree-ring datasets: 2500 years of reconstructed temperature and precipitation anomalies (Dendro 2500) and 1250 years of reconstructed temperature and precipitation anomalies (Dendro 1250). The tree-ring series were compared to climate observations to statistically identify the best temporal fit: Correlation coefficient *r* was determined with altering monthly combinations also considering pervious year measurements. Once the highest correlation has been determined, it is assumed that the tree-ring series represent seasonal precipitation or temperature patterns (i.e. AJJ, JJA or JJAS) within the entire chronology.

2.2 The Hydrological Modelling System PREVAH

2.2.1 Model Description

The hydrological modelling system PREVAH (PREcipitation-Runoff-EVApotranspiration-HRU model) is based on the HBVs model structure (Viviroli et al. 2009). The well-known HBV (Hydrologiska Byråns Vattenbalansavdelning) model has a long history in hydrological modelling and has been applied in numerous studies in more than 30 countries (Lindström et al. 1997; Seibert 1997). The HBV model is classified as a semi-distributed conceptual model and consists of three main components: Submodules for snow accumulation and snow melt; submodules for soil moisture computation; response functions and river routing submodules (Bergström & Singh 1995). The emerged PREVAH model is also a semi-distributed conceptual model with implemented hydrological similar response units (HRU's) and was originally developed to understand the spatial and temporal variability of hydrological processes in mountainous catchments with complex topography (Viviroli et al. 2009). HRUs, or hydrotopes, are spatially distributed grid-cells covering a catchment that exhibit hydrological similar behavior (Gurtz et al. 1999) in contrary to uniform raster-cells (Viviroli et al. 2009). PREVAH consists of several subsystems such as anticipated submodules for interception, soil water storage and depletion by evapotranspiration, runoff and baseflow generation, discharge concentration and flood-routing, and specific submodules to represent mountainous catchments such as snow accumulation, snow melt and glacial ice melt (Viviroli et al. 2009).

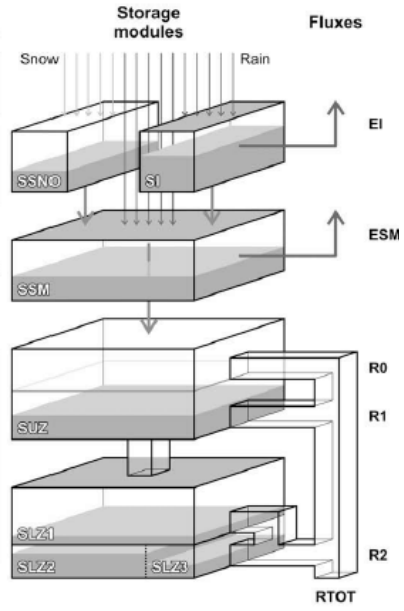

Figure 2: Schematic of PREVAHs runoff generation.

Source: Viviroli et al. (2009): 1212

The total runoff generation (RTOT) is based on the HBVs model concept with three vertical runoff components: Quick (R0), delayed (R1) and slow (R2) runoff (Viviroli et al. 2009). EI stands for evaporation from interception storage and ESM stands for evapotranspiration from soil moisture storage. Under consideration of parameterized soil characteristics, the runoff generation in the unsaturated zone (SUZ) depends on the storage time for surface runoff and interflow. In the saturated zone (SLZ), the baseflow is

determined by two groundwater reservoirs with a quick and delayed runoff component. The computed storage threshold regulates the generation of the total surface runoff considering percolation rates, storage limits and flux regulations.

In this thesis a specific version of PREVAH was used which has been successfully validated for all major Swiss rivers and streams by Zappa et al. (2012) with a spatial resolution of 200 x 200 m as well as land use and soil type information for HRU classification. Even though PREVAH usually computes at an hourly time-step, only annually and monthly resolved cycles were modelled, mainly due to computation limits.

2.2.2 Input Parameters

Besides physiographical information for the HRUs such as land use and soil type, the PREVAH model requires meteorological input parameters for computation, namely temperature, precipitation, sunshine duration, cloud cover, relative humidity and wind speed (Viviroli et al. 2009). The temperature and precipitation reconstructions are included into a calibrated meteorological database, extending the temporal resolution beyond instrumental observations ranging from (a) 500 B.C. to 2012 A.D. and (b) 760 A.D. to 2012 A.D. As for sunshine duration, cloud cover, relative humidity and wind speed, no proxy-based estimate was available. To overcome this gap of missing information, calibrated model estimates based on the calibration period from 1971 to 2012 were used. The calibrated information was hence randomly distributed 21 times and joint to each non-randomly distributed temperature and precipitation dataset resulting in 21 files with randomly distributed sunshine duration, cloud cover, relative humidity and wind speed information of the calibration period 1971 to 2012 and chronologic temperature and precipitation estimates. To evaluate the models accuracy, the actual non-randomly distributed pre-settings for sunshine duration, cloud cover, relative humidity and wind speed were used ascending from 1971 to 2012. It is however noteworthy that the model itself has tuneable parameters which were calibrated for the total runoff generation during the time period of 1984 to 2012. Subsequently, all of the runoff analysis is focused within the time period of 1984 to 2012.

2.2.3 Output

Numerous variables are computed based on the models core parameters (Vviroli et al. 2009):

(a) Water sources: Volume corrected precipitation, snow melt and ice melt.

(b) Storages: Snow storage, interception storage, soil moisture storage, upper (unsaturated) zone runoff storage and lower (saturated) zone runoff storage.

(c) Fluxes: Quick runoff, delayed runoff, slow runoff, total runoff, evapotranspiration from interception storage and evapotranspiration from soil moisture storage.

The potential evapotranspiration is calculated using the Penman equation and the actual evapotranspiration is calculated using the Penman-Monteith equation (Gurtz et al. 1999). Also, the loss of water due to evapotranspiration and runoff is given by the total amount of water available for runoff and soil based on the magnitude of the water source, flux and storage units (Gurtz et al. 1999). Basically, all of the computation steps including fluxes and storage units serve to generate the total runoff, probably the most important output variable in hydrological modelling.

2.2.4 Catchments

Two catchments were selected to represent the Swiss Midland and the Swiss Alpine environment: The Murg stream and the Dischmabach stream.

(a) The Murg catchment covers a surface of 78.9 km^2, has a mean elevation of 650 m a.s.l. with no glaciation. The river gauge is situated by Waengi in the canton of Thurgau at 47° 29' N and 8° 57' E.

(b) The Dischmabach catchment covers a surface of 43.3 km^2, has a mean elevation of 2372 m a.s.l. with 2.1% areal glaciation. The river gauge is situated by Kriegsmatte near Davos in the canton of Graubuenden at 46° 46' N and 9° 52' E.

For both catchments the Dendro 2500 and the Dendro 1250 datasets were used thus both files comprise temperature reconstructions from different locations with the same precipitation reconstructions (see chapter 2.1.2 and 2.1.3)

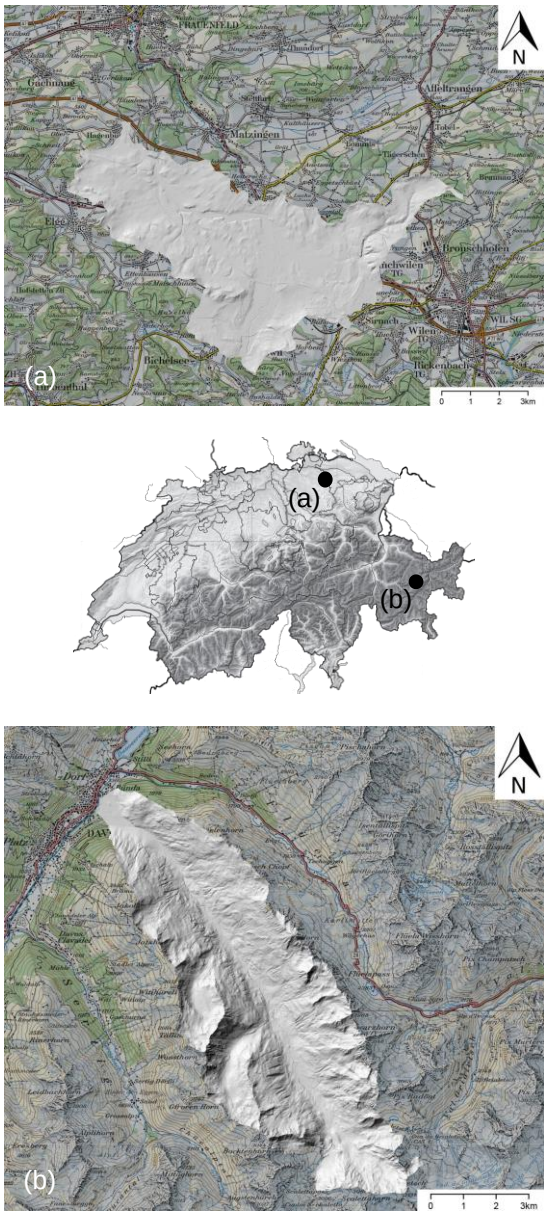

Figure 3: The Murg (a) and the Dischmabach (b) catchments.

Source: SwissTopo ©

2.2.5 Glacier Mass Balance

In glaciology, the difference between the accumulation of ice mass through snow densification in the accumulation area and the loss of ice mass in the ablation area is referred to as mass balance (Benn & Lehmkuhl 2000). Based on this general definition an idealistic glacier mass balance model has been established based on the modelled snow storage (accumulation) and ice melt (ablation). At the moment, 2.1% of the Dischmabach catchment is covered by the Scaletta glacier. The established mass balance model can hence be applied for the Dischmabach catchment:

$$\boldsymbol{b = acc - abl} \quad (1)$$

b is the mass balance, *acc* is the modelled snow accumulation and *abl* is the modelled ice ablation. According to Hoelzle et al. (2007), the potential annual length variations ΔL can also be estimated using equation 2:

$$\boldsymbol{\Delta L = \frac{\Delta b}{A}} \quad (2)$$

L_0 is the initial, observable length of the Scaletta glacier, Δb is the mean mass balance variation over one year and *A* is the annual ablation. The modelled absolute length *L* for the Scaletta glacier is hence:

$$\boldsymbol{L = L_0 + \Delta L} \quad (3)$$

It is noteworthy that the mass balance and the length change models are a very idealistic, two-dimensional approach not considering the hillslope, the glaciers thermal regime or other feedback interactions (e.g. response time).

2.3 Instrumental Data

In order to assess the validity of the results, the tree-ring measurements as well as the output from the hydrological modelling system PREVAH were compared with instrumental observations for statistical evaluation.

2.3.1 Climatic Data

Mean monthly temperature anomalies [°C] and mean monthly precipitation sum anomalies [%] from HISTALP high- (>1500 m a.s.l.) and HISTALP low-elevation (<1500 m a.s.l.) were used to detect and evaluate climatic signals within the tree-ring series. The HISTALP database consists of monthly homogenized climatic data for the Greater Alpine Region with temperature time series extending back to 1760 A.D. and precipitation time series extending back to 1800 A.D. Within the Greater Alpine Region, numerous international monitoring stations measuring air temperature, air pressure, precipitation, sunshine and cloudiness are scattered over a surface of approximately 714'000 km^2. The HISTALP database maintains climate data of each monitoring station within the Greater Alpine Region which were classified into regions with common climate variation, also referred to as the Coarse Resolution Subregions (CRS). CRS were selected after optimized regionalization procedures using principle

component analysis (PCA) and empirical orthogonal functions (EOFs) in two dimensions were applied. As the HISTALP dataset also comprises high vertical climate variability, additional subgroups for high-elevation sites (>1500 m a.s.l.) were formed. The results are monthly homogenized and regionalized climate datasets and as all of the HISTALPs CRS files have undergone regionalization procedures over a greater spatial scale, it should not be neglected that the series deflects lower frequency analysis as compared to non-homogenized one-station observations (Auer et al. 2007).

Mean monthly temperatures [°C] and mean monthly precipitation sums [mm] from four reliable MeteoSwiss stations (Basel-Binningen, Geneva-Cointrin, Bern-Zollikofen and Zurich; according to Schaer et al. 2004) were grouped. The average values of all four MeteoSwiss stations were used to further detect and evaluate climatic signals within the tree-ring series. Similar to HISTALP, MeteoSwiss consists of 12 homogenized precipitation and temperature time series extending back to 1864 A.D. (Begert et al. 2005). Different from HISTALP, other homogenization procedures were applied.

2.3.2 Runoff Data

Mean annual and mean monthly runoff data [m^3/s] from the Swiss Federal Office for the Environment (FOEN) was used to evaluate the simulated total runoff. Annual runoff data from the river gauge Waengi (Murg) from 1914 to 2012, annual runoff data from the river gauge Kriegsmatte, Davos (Dischmabach) from 1981 to 2012, monthly runoff data from the river gauge Waengi (Murg) from 1914 to 2009 and monthly runoff data from the river gauge Kriegsmatte, Davos (Dischmabach) from 1981 to 2009 were used for statistical evaluation.

2.3.3 Glacier Data

To assess the glacier length model, observed length changes for the Scaletta glacier and the Silvrettaglacier from the Swiss Glacier Network VAW/ETHZ & EKK/SCNAT were used. The patchy dataset for the Scaletta glacier ranges from 1895 to present. The Silvrettaglacier lies approximately 17 km northeast of the Scaletta glacier with annual measurements from 1956 to present. Unfortunately, no data for the mass balance was available.

2.4 Other Proxy Records

A 1200 year long drought reconstruction based on carbon isotope measurements from tree-ring series in the Swiss Alps (Loetschental and Simplon village, canton of Valais) was provided by Dr. Ulf Buentgen with the consent of Dr. Anne Kress (Kress et al. 2014). The drought index (DRI) ranging from 800 A.D. to 2004 A.D. was calculated by Kress et al. (2014) according to Thornthwaite (1948) and further converted into z-scores:

$$\boldsymbol{DRI = P - PET} \tag{4}$$

P is monthly precipitation and *PET* monthly potential evapotranspiration. The DRI was standardized to the mean value μ in relation to the standard deviation σ (Kress 2009):

$$\boldsymbol{DRIz = \frac{DRI - \mu}{\sigma}} \tag{5}$$

The DRI_z was then compared with z-scores from a simulated drought index (DRI_s) and the modelled plant available soil moisture storage (SSM).

2.5 Statistical Analysis

2.5.1 Tree-Ring Data

The tree-ring chronologies were detrended to remove non-climatic, age-related growth trends using the Regional Curve Standardization (RCS) method and further converted into anomalies (Buentgen et al. 2006; Buentgen et al. 2011). As the tree-ring data was provided by Dr. Ulf Buentgen, only Pearson's correlation coefficient *r* and a Pearson's coefficient of determination R^2 were determined if the given datasets were Gaussian distributed. To determine if the data was Gaussian distributed, a Shapiro-Wilk normality test was performed (p-value > 0.05). If the data was not Gaussian distributed, Spearman's correlation coefficient was determined. The tree-ring series were further compared with HISTALP high-elevation, HISTALP low-elevation and MeteoSwiss temperature and precipitation anomalies to determine the best statistical fit.

2.5.2 Hydrological Model Evaluation – Simulated Runoff

Before interpreting the simulated results, any hydrological modelling system has to be evaluated to distinguish, whether the simulations are sufficiently accurate or not (Moriasi et al. 2007). According to Moriasi et al. (2007), performance ratings are model and project specific, but they can emphasize whether the model should be accepted or rejected. Unfortunately, at a later stage of this project, an internal model error was identified. Fact is that the model computed false volume-corrected precipitation which automatically induced an aftereffect on all of the other model parameters. Therefore no statistical test regarding absolute values such as the Nash-Sutcliffe efficiency, a normalized statistic to determine the relative magnitude between the simulated variance and the observed variance (Nash & Sutcliffe 1970), the percent bias (PBIAS), a statistic which estimates the average tendency of the simulated data to be larger or smaller than the observed data (Gupta et al. 1999), mean square error (MSE), root mean square error (RMSE), mean absolute error (MAE), the index of agreement (d) (Legates & McCabe 1999) and the root mean square error-observations standard deviation ratio (RSR) (Moriasi et al. 2007) were conducted because the results would have been biased due to the internal error.

Nevertheless, Pearson's correlation coefficient *r* and Pearson's coefficient of determination R^2, which describe the degree of collinearity between simulated and observed data (Moriasi et al. 2007), were determined as long the output was Gaussian distributed. To determine if the data was Gaussian distributed, a Shapiro-Wilk normality test was performed (p-value > 0.05). If the data was not Gaussian distributed, Spearman's correlation coefficients were determined.

The statistical analyses were conducted for an overall average of the 21 datasets deflecting a natural variability and for each dataset individually. The best results are shown in table 2.

2.5.3 Glacier Mass Balance & Length Changes

The results for the glacier mass balance model were visually compared with other Swiss Alpine glacier advance figures to evaluate, if similar reconstructed trends are visually detectable. No numeric data for mass balances were available for the Scaletta glacier. The modelled length change for the Scaletta glacier was compared with length change observations for the Scaletta glacier and the Silvrettaglacier thus the dataset for the Scaletta glacier exhibited a range of missing values.

Subsequently, Pearson's correlation coefficient *r* and coefficient of determination R^2 were determined if the data was Gaussian distributed. To determine if the data was Gaussian distributed, a Shapiro-Wilk normality test was performed (p-value > 0.05). If the data was not Gaussian distributed, Spearman's correlation coefficients were determined.

2.5.4 Other Proxy Records

Pearson's correlation coefficient *r* and Pearson's coefficient of determination R^2 were determined to compare the drought index (DRI_z) from Kress et al. (2014) with the modelled drought indices (DRI_s, SSM) as long as the data was Gaussian distributed. To determine if the data was Gaussian distributed, a Shapiro-Wilk normality test was performed (p-value > 0.05). If the data was not Gaussian distributed, Spearman's correlation coefficients were determined.

3. Results

3.1 Tree-Ring Data

3.1.1 Precipitation

The precipitation tree-ring series was compared with monthly instrumental precipitation data from HISTALP high, HISTALP low and MeteoSwiss. Highest correlations were determined for the April-June-July time period (r = 0.27) comparing the anomalies with the homogenized MeteoSwiss datasets ranging from 1864 to 2012 A.D.

3.1.2 Temperature

Both temperature tree-ring series were compared with monthly instrumental temperature data from HISTALP high, HISTALP low and MeteoSwiss.

(a) The highest correlation coefficient for Dendro 2500 was determined for the June-July-August time period (r = 0.66).
(b) The highest correlation coefficient for Dendro 1250 was determined for the June-July-August-September time period (r = 0.72).

Highest correlations for both temperature tree-ring series were scored comparing the anomalies with the homogenized MeteoSwiss datasets ranging from 1864 to 2012 A.D.

	Dendro 1250 JJAS Temperature		Dendro 2500 JJA Temperature		Dendro 2500 AMJ Precipitation	
	r	R^2	r	R^2	r	R^2
HISTALP High	0.7	0.49	0.59	0.35	-	-
HISTALP Low	0.68	0.46	0.6	0.36	0.14	0.02
MeteoSwiss	0.72	0.52	0.66	0.44	0.27	0.07

Table 1: Comparsion of tree-ring series with instrumental data.

3.2 Hydrological Model Evaluation

In the following sections, the simulated runoff is statistically compared with instrumental data. Ascending from 1971 to 2012 the models calibrated pre-settings for sunshine duration, cloud cover, relative humidity and wind speed were used. The

tuneable parameters for the total runoff generation were calibrated from 1984 to 2012.

3.2.1 Simulated Runoff

(a) The results computed for the Murg stream were compared with instrumental runoff observations from (i) 1914 to 1984 and (ii) during the calibration period from 1984 to 2009/2012. Between 1918 and 1921 and between 1936 and 1953 no observed runoff data was available. Pearson's correlation coefficients *r* varies between (i) 0.24 and 0.37 with 5% to 14% variance explained and (ii) 0.78 and 0.92 with 60% to 85% variance explained in which the monthly simulations scored higher than the annual simulations.

(b) The results for the Dischmabach stream were compared with instrumental runoff observations from (i) 1981 to 1984 and (ii) 1984 to 2009/2012. Since no data prior to 1981 was available, model performance statistics outside the calibration period was only conducted over 4 years and should hence be interpreted cautiously. Pearson's correlation coefficient *r* varies between (i) 0.94 and 0.98 with 82% to 96% variance explained and (ii) 0.42 and 0.94 with 15% to 88% variance explained in which the monthly simulations scored higher than the annual simulations.

In all model runs the total runoff was underestimated in which the monthly simulations scored higher than the annual simulation. The correlation coefficient and coefficient of determination show good results during the calibration period, but indicate poor results outside the calibration period. Since model performance statistics for the Dischmabach stream outside the calibration period were only conducted over 4 years, the calculated results can be neglected because the number of comparable observations vs. simulations is too small.

Catchment	Tree-Ring Dataset	Temporal Resolution	Simulated Runoff	
			r	R^2
Murg*	Dendro 2500	Annual	0.24	0.05
Murg*	Dendro 2500	Monthly	0.37	0.14
Murg*	Dendro 1250	Annual	0.35	0.11
Murg*	Dendro 1250	Monthly	0.35	0.12
Dischmabach*	Dendro 2500	Annual	0.94	0.83
Dischmabach*	Dendro 2500	Monthly	0.98	0.95
Dischmabach*	Dendro 1250	Annual	0.94	0.82
Dischmabach*	Dendro 1250	Monthly	0.98	0.96

Catchment	Tree-Ring Dataset	Temporal Resolution	Simulated Runoff	
			r	R^2
Murg	Dendro 2500	Annual	0.78	0.60
Murg	Dendro 2500	Monthly	0.92	0.85
Murg	Dendro 1250	Annual	0.78	0.60
Murg	Dendro 1250	Monthly	0.92	0.85
Dischmabach	Dendro 2500	Annual	0.42	0.15
Dischmabach	Dendro 2500	Monthly	0.94	0.88
Dischmabach	Dendro 1250	Annual	0.42	0.15
Dischmabach	Dendro 1250	Monthly	0.94	0.88

** 1914 - 1984 for the Murg; 1981 - 1984 for the Dischmabach*

Table 2: Simulated runoff evaluation.

3.2.2 Glacier Mass Balance

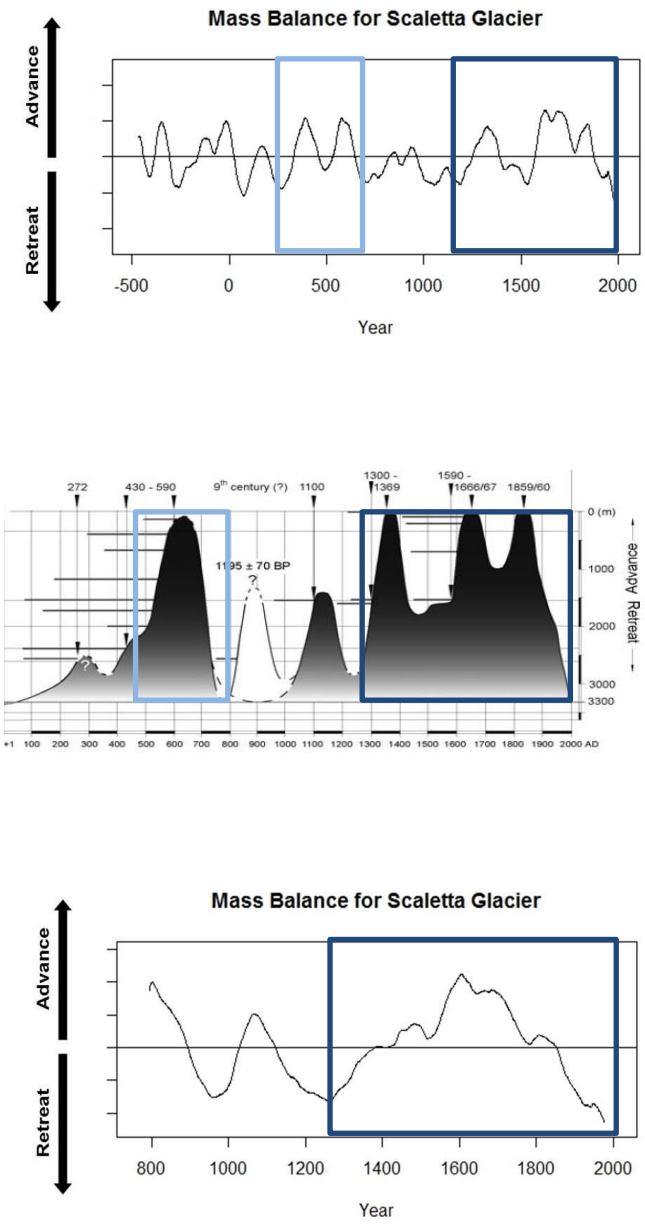

Figure 4: Visual comparison of glacier mass balance models for Swiss glaciers.

The first figure shows the modelled 2500 year reconstruction, the second figure shows a reconstruction for the Great Aletsch glacier (Holzhauser et al. 2005: 791) and the third figure shows the modelled 1250 year reconstruction.

The idealistic glacier mass balance model was applied for the Dischmabach catchment using both Dendro 2500 and Dendro 1250 datasets thus 2.1% of the surface area is covered by the Scaletta glacier. Unfortunately, no absolute values for the mass balance of the Scaletta glacier are available to compare them with the simulated fluctuations. Therefore only a visual assessment was possible. A 50 year filter was applied for the modelled mass balance to compare it with figures of European glacier variations from Holzhauser et al. (2004). Holzhauser et al. (2004) used historical and archeological material to reconstruct the last 450 years and used fossil soils (palaeosols) and wood fragments to establish a chronology of glacier fluctuations throughout the entire Holocene using the radiocarbon dating method from numerous sources. Both paleosols and fossil woods were dated using the radiocarbon method with an accuracy of 100-200 years (Holzhauser et al. 2004). Even though the magnitude of glacier advances and retreats are unknown,

both reconstructed glacier variation figures show similarities with the modelled results which indicate that the model is not entirely bad.

The simulated length change was compared with observed values for the Scaletta glacier and the Silvrettaglacier. While the comparison of the simulated and observed length change for the Scaletta glacier showed negative correlations for the time period 1895 to 2012, high positive values were scored during the calibration period 1984 to 2012. The comparison of the simulated length change for the Scaletta glacier and the observed length changes for the Silvretta also showed promising high correlations.

				Absolute Length Change	
Catchment	Tree-Ring Dataset	Temporal Resolution	Simulated vs. Observed Glacier	r	R^2
Dischmabach*	Dendro 2500	Annual	Scaletta/Scaletta	0.42	0.11
Dischmabach*	Dendro 1250	Annual	Scaletta/Scaletta	0.41	0.10

				Absolute Length Change	
Catchment	Tree-Ring Dataset	Temporal Resolution		r	R^2
Dischmabach	Dendro 2500	Annual	Scaletta/Scaletta	-0.61	0.36
Dischmabach	Dendro 1250	Annual	Scaletta/Scaletta	-0.55	0.29

				Absolute Length Change	
Catchment	Tree-Ring Dataset	Temporal Resolution	Simulated vs. Observed Glacier	r	R^2
Dischmabach*	Dendro 2500	Annual	Scaletta/Silvretta	0.56	0.28
Dischmabach*	Dendro 1250	Annual	Scaletta/Silvretta	0.54	0.26

				Absolute Length Change	
Catchment	Tree-Ring Dataset	Temporal Resolution		r	R^2
Dischmabach	Dendro 2500	Annual	Scaletta/Silvretta	0.52	0.26
Dischmabach	Dendro 1250	Annual	Scaletta/Silvretta	0.50	0.23

** 1984 - 2012*

Table 3: Comparison of simulated and observed length changes.

The simulated length change for the Scaletta glacier was compared with the observed length change for the Scaletta glacier (upper) and with the observed length change for the Silvrettaglacier (lower).

3.3 Other Proxy Records

Catchment	Tree-Ring Dataset	Temporal Resolution		DRI r	DRI R^2
Murg	Dendro 2500	Annual	DRI_S	-0.03	0.00
Murg	Dendro 2500	Annual	SSM	-0.06	0.00
Murg	Dendro 2500	Monthly	DRI_S	-0.02	0.00
Murg	Dendro 2500	Monthly	SSM	0.04	0.00
Murg	Dendro 1250	Annual	DRI_S	-0.01	0.00
Murg	Dendro 1250	Annual	SSM	-0.03	0.00
Murg	Dendro 1250	Monthly	DRI_S	-0.03	0.00
Murg	Dendro 1250	Monthly	SSM	-0.09	0.01
Dischmabach	Dendro 2500	Annual	DRI_S	-0.06	0.00
Dischmabach	Dendro 2500	Annual	SSM	-0.02	0.00
Dischmabach	Dendro 2500	Monthly	DRI_S	-0.03	0.00
Dischmabach	Dendro 2500	Monthly	SSM	-0.01	0.00
Dischmabach	Dendro 1250	Annual	DRI_S	0.01	0.00
Dischmabach	Dendro 1250	Annual	SSM	0.02	0.00
Dischmabach	Dendro 1250	Monthly	DRI_S	-0.03	0.00
Dischmabach	Dendro 1250	Monthly	SSM	-0.04	0.00

Table 4: Comparison of drought indices.

The drought index by Kress et al. (2014) was compared with the z-scores of the modelled drought index (DRI_S) and the modelled plant available soil moisture storage (SSM). Correlation coefficients range between -0.09 and 0.04 and both comparisons are equally statistically insignificant. However, a temporal lag between the Kress et al. (2014) DRI and the modelled DRI_S/SSM is noticeable (see appendix). Unfortunately, the lag is not prominent enough to increase the statistical significance (r = 0.04).

4. Discussion

This chapter is divided into two parts: Part A discusses the results based on the evaluated statistics from chapter 3. Part B discusses selected paleohydroclimatic events and emphasizes that hydroclimatological trends were detected.

Part A - Statistical Evaluation

4.1 Tree-Ring Data

4.1.1 Tree-Rings

The highest correlation for the April-June-July precipitation reconstruction was achieved comparing the tree-ring series with instrumental data from MeteoSwiss (r = 0.27). The highest correlation for both the June-July-August (r = 0.66) and the June-July-August-September (r = 0.72) temperature reconstructions were also achieved comparing the tree-ring series with instrumental data from MeteoSwiss. A correlation coefficient of 0.27 is poor and the null hypothesis should be rejected. However, a correlation coefficient of 0.66 and 0.72 is high.

Tree growth and the development of annual tree-rings are influenced by numerous environmental factors such as precipitation, temperature, elevation, exposure, geologic and pedologic properties and subsequent plant available nutrients, interactions with flora and fauna as well as anthropogenic influences (Fritts 1976). Therefore a variety of environmental signals are preserved in tree-rings and it is nearly impossible to detect one climatic signal without any additional noise. Another important point is that trees react to environmental stresses differently, either direct or delayed. For example, if a tree suffers from short-term water stress during the growing season, the tree-ring growth is decelerated. If a tree suffers from long-term water stress, the tree-ring growth is stopped and the tree might succumb to hydraulic failure or carbon starvation (McDowell et al. 2008; McDowell 2011). During extreme and prolonged drought stress, the severity of the drought stress affecting the tree growth cannot be estimated without uncertainties. In some cases as in the Mediterranean for instance, mid-summer droughts occur frequently interfering with

tree-ring growth. Mediterranean trees and shrubs often form inter-annual bands of latewood, also referred to as false rings, associated with mid-summer droughts that can falsify the dating (Copenheaver et al. 2010). In such cases, no accurate allocation of years is possible and any comparison with instrumental data would be pointless. In short, physiological mechanisms how trees react to prolonged drought stresses are still uncertain.

The law of limiting factors and the concept of ecological amplitude need to be considered reconstructing any climate signal, construing the importance of selecting the to-be sampled species and the sampling site (Fritts 1976). The precipitation for instance was reconstructed based on precipitation-sensitive oak (*Quercus* L.) tree-ring width series in northeastern France as well as in north- and southeastern Germany (Buentgen et al. 2011). Oak tree-ring chronologies, reconstructing spring precipitation, have been applied in numerous studies before achieving statistically significant results with *r* ranging between 0.52 and 0.69 (Akkemik et al. 2005) or ranging between 0.22 and 0.57 (Griggs et al. 2007). Buentgen et al. (2011) also achieved higher correlations with *r* ranging between 0.37 and 0.53 when compared to precipitation data from northeastern France, north- and southeastern Germany. So, if we exclude that oak tree-ring series are not suitable for reconstructing precipitation anomalies, then we should take a closer look into the sampling sites: The tree-ring series was compiled from subfossil, archeological, historical and recent material in northeastern France, north- and southeastern Germany (Buentgen et al. 2011). The anomalies were compared with instrumental data from the Greater Alpine Region (HISTALP) and with instrumental data from Switzerland (MeteoSwiss). The homogenized HISTALP and MeteoSwiss datasets contain high climatic variability (Wanner et al. 1997; Auer et al. 2007) and it could therefore be debated, if spatially scattered tree-ring series over the Greater Alpine Region can be compared to spatially confined precipitation data. Though better statistical results were conducted when comparing the data to the MeteoSwiss dataset, it clearly makes sense to compare the proxy signal with available instrumental data near the sampling sites. This would label the samples spatially and should hence not be implemented into a hydrological modelling system for any Swiss catchments. Unfortunately, no tree-ring data with remarkable temporal resolution for the Murg and the Dischmabach catchments were available.

The growing season, defined as the time in which trees grow due to optimal climatic conditions, is highly variable in both space and time (Fritts 1976). In the temperate deciduous forest biome, the growing season starts between March/April, when air temperatures start to increase and ends towards September/October, when air temperatures start to decrease, for 5 to 6 months (Chiras 2013). It is therefore impossible to detect climate signals that represents an entire annual cycle and only signals during the growing season can be detected. The climate of the prior growing period also exerts a great influence on tree growth and can influence later tree-rings growth (Fritts 1976), suggesting that previous year anomalies might also influence later tree-ring growth.

As a final point of criticism, the standardization process could also be scrutinized: Biological and age related growth trends are generally visible throughout a trees life making the standardization process a necessity (Fritts 1976; Helama et al. 2004). Helama et al. (2004) or Bunn et al. (2004) discuss which standardization procedure is best and conclude that for long tree-ring chronologies with low-frequency variations, the Regional Curve Standardization (RCS) method is robust to detrend age-related growth trends if the requirements can be met. Therefore we assume that the standardization process had no influence on the statistical results.

4.2 Hydrological Model Evaluation

4.2.1 Runoff

According to Moriasi et al. (2007), hydrological model performance ratings are model and project specific. This thesis tries to investigate if past hydrological cycles can be modelled by implementing precipitation and temperature reconstructions based on tree-ring series into the hydrological modelling system PREVAH. Due to an unexpected internal model error, the volume corrections were falsely computed preventing any statistical model evaluation based on absolute values. Therefore only correlation coefficients and coefficients of determination were evaluated.

Correlation coefficients *r* range between 0.24 and 0.37 for the Murg catchment and range between 0.94 and 0.98 for the Dischmabach catchment outside the calibration period. During the calibration period from 1984 to 2012, correlation coefficients *r* range between 0.78 and 0.92 for the Murg catchment and 0.42 and 0.94 for the

Dischmabach catchment. Generally, correlation coefficients indicate low correlation outside the calibration period and high during the calibration period.

From a modelling perspective, both catchments exhibit poor model performance outside the models calibration period. However, comparing the modelled result from both catchments within the calibration period, the models performance is rather good, especially for the monthly performances. Based on the first results, it seems feasible to model total runoff if the model can be calibrated. The calibration procedure includes accurate information on land use and land use change, soil type, sunshine duration, cloud cover, relative humidity and wind speed as well as rough adjustments of the tuneable parameters. Unfortunately, there is neither information covering the last 1250 nor the last 2500 years. This idealistic approach however could have achieved better statistical results if the precipitation reconstructions were better. Because of an internal model error, it is unrealistic and unfair to judge the models performance regarding the randomly distributed pre-settings.

Regarding the models internal error, the simulated runoff was most likely underestimated because the model computed false volume corrections adding either less or more deviations (deltas) to the observational database inducing an aftereffect on the total runoff generation. Before repeating this model set-up, the internal error should be identified and fixed. Subsequently, no actual statistical statement can be made whether the model set-up using tree-ring based climate reconstructions and randomly distributed pre-settings was successful and our results should be hence interpreted as a first attempt.

4.2.2 Glacier Mass Balance

No statistical test was performed for the mass balance model because no absolute values for the mass balance were available. Comparing the modelled mass balance with figures of European glacier variations suggests good model performance.

The simulated length change of the Scaletta glacier was compared to observed values of the Scaletta glacier and the Silvrettaglacier. Comparing the modelled results with observed length changes for the Scaletta glacier, correlation coefficients show a high negative correlation for the time period 1895 to 2012. Within the calibration period 1984 to 2012 the correlation is positive with moderate statistical

significance. There are numerous reasons why the correlation is poor and even inverse: The models setup is highly idealistic neglecting the thermal regime, the hillslope and the glaciers response time implying a wrong temporal allocation of advances and retreats. A glaciers response time is the time a glacier needs to adjust its geometry to a climate change signal (Raper & Braithwaite 2009). The response time is dynamic in a sense that a climate disturbance has a long-term effect on the glaciers geometry including its length. Therefore a glacier does not react to a climate signal direct but delayed. This important fact was neglect in our model. Another point is the models internal error resulting in false absolute values inducing wrong magnitudes of glacier length changes. However, the magnitude of the models computed values has no effect on correlation coefficients.

When comparing the simulated length change for the Scaletta glacier with the observed length changes for the Silvrettaglacier, the results show exceptionally good results with *r* between 0.5 and 0.52 for the time period 1956 to 2012 and *r* between 0.54 and 0.56 during the calibration period. The Silvrettaglacier lies approximately 17 km northeast of the Scaletta glacier and is one of the best observed Swiss glaciers. Obviously, the magnitudes of the length changes differ (and not only because of the models internal error), but the correlation remains high. The precipitation and the temperature reconstructions comprise high climatic variability making it plausible for the results to show similarities with regional observations. Unfortunately, the glacier length simulation within the Dischmabach catchment shows moderate results, but due to the fact that the results are high for the Silvrettaglacier it is considerable to highlight the models performance detecting regional trends.

4.2.3 Other Proxy Records

The drought index (DRI) by Kress et al. (2014) was compared with the modelled drought indices (DRI_S, SSM). Correlation coefficient *r* ranges between -0.09 and -0.01 for the Murg catchment and -0.06 and 0.02 for the Dischmabach catchment indicating no correlation. However, it seems that the DRI lags the modelled drought indices. One possible reason for the temporal lag could be the problem of drought definition:

According to Dracup et al. (1980) and Wilhite and Glantz (1985), meteorological droughts describe dry atmospheric conditions with precipitation deficiencies. Agricultural drought describes soil water deficiencies affecting crop growth, often

linked to both meteorological and hydrological drought. Hydrological droughts describe low runoff and depleted water storage reservoirs and usually lag the occurrences of meteorological and agricultural droughts. The temporal lag would be explained if the DRI from Kress et al. (2014) would be considered as hydrological drought. The DRI however is defined as precipitation minus potential evapotranspiration and can hence be attributed to agricultural drought. A temporal lag is therefore not explained considering drought definitions itself. But, if agricultural drought is affected by both meteorological and hydrological drought, precipitation deficiencies may not affect tree growth directly, but the lagged depleted soil storage reservoirs could stress the tree in following years. This could, if the drought duration is long enough, cause a temporal lag of a few years in the drought reconstruction depending on the trees recovery time.

Another possibility is that water stress affects tree growth either directly or delayed. When a long-term drought occurs, the tree might succumb to hydraulic failure or carbon starvation interfering with inter-cellular carbon contents, or cells might even fracture due to hydraulic failure (McDowell et al. 2008; McDowell 2011). If cells fracture due to declining leaf water potentials, the recorded drought signal should be simultaneous with the water deficiency, but the trees recovery time might artificially extend the actual drought duration. This would not explain a temporal lag, but rather a differentiation on drought durations. If trees prohibit stomatal conductance, no additional carbon will be produced and depending on drought duration, carbon storages will be depleted. This effect, also known as carbon starvation, could cause a temporal lag in the tree-ring series. Another critical point regarding carbon starvation is that carbon starvation occurs over long drought episodes (McDowell et al. 2008). If long drought episodes force the tree to prohibit stomatal conductance and carbon storage depletion, then any analysis on carbon concentrations within tree-rings is questionable, thus it is still unknown how the carbon storages are replenished and how carbon starvation affects post-stress carbon re-distribution. Trees might be much more sensible to any water stress occurring after a major drought event distorting the entire drought record. However, up to date there is little evidence to support the hypothesis of carbon depletion due to drought stress in trees (Sala 2009; Anderegg 2012) and if evidence is present, only in very few instances substantiating the fact that the effect of drought-stress on tree-rings is still a matter of debate and should hence be interpreted cautiously.

Overall, no statement can be made on which drought reconstruction is more accurate since both drought reconstructions have not been compared with other known drought records.

Part B – Paleohydroclimatic Trends

4.3 Paleohydroclimatic Trends

4.3.1 Roman Climate Optimum

It is generally accepted that more than 2000 years ago, North African, Mediterranean and central European climate was warmer and moister than todays (Reale & Dirmeyer 2000). During the height of the Roman imperium, multiple proxy records indicate increased temperatures between ~ 300 B.C and 400 A.D. which is why this time period is referred to as Roman Climate Optimum (Hass 1996).

The reconstructed temperature record indicates that the Roman Climate Optimum was ~ 0.4°C higher than the reference period from 1901 to 2000, and reconstructed precipitation indicates an increase by ~ 2%. The simulated runoff also shows increased runoff as compared to the reference period, but since the absolute runoff is generally underestimated, no statement on the magnitude can be made. The modelled glacier mass balance for the Scaletta glacier is predominately negative suggesting glacier retreat, being in coherency with other proxy records. When looking at the modelled drought indices, no pronounced drought can be detected indicating higher precipitation than potential evapotranspiration rates deflecting the hypothesis of a moister climate.

4.3.2 Medieval Warm Period

The so called Medieval Warm Period (MWP) ~ 1000 A.D. to 1300 A.D. has been a matter of debate ever since it was first described in 1965 by Lamb. While for instance Hughes and Diaz (1994) emphasize a lack of evidence for its occurrence, other scientists found increasing proof that mean global temperatures were elevated supporting the theory of a global MWP (e.g. Cook et al. 2002; Esper et al. 2005).

The temperature reconstructions indicate ~ 0.8°C lower temperatures than the 1901 to 2000 reference period, and the precipitation was decreased by ~ 1%. Again, no statement on the magnitude of the simulated total runoff can be made thus the simulated runoff is underestimated. The precipitation however shows a noticeable decrease between 1150 and 1200 A.D. and is confirmed by the simulated drought indices as well as by the drought index by Kress et al. (2014). The glacier mass

balance reaches a negative peak at 1150 A.D. indicating increased glacial ice melt, but shifts towards positive values after 1200 A.D.

Based on the proxy records and the simulated results, no clear statement can be made whether a warm episode occurred supporting the hypothesis of a Medieval Warm Period. However, our data suggests that between 1000 and 1200 A.D. a pronounced drought occurred with precipitation deficits and increased glacial ice melt. The increased ice melt could have been caused by elevated mean annual air temperatures, but also by less snowfall decreasing accumulation rates. It is generally accepted that during the last 1000 years frequent droughts occurred in the northern hemisphere with pronounced precipitation deficits (Stanley 2009) supporting the idea of less snowfall. Geochronological studies in the Swiss Alps also suggest that Swiss glaciers retreated until ~ 1200 A.D. (Broecker 2001; Holzhauser et al. 2005) being in coherency with the modelled mass balance amplifying our hypothesis. However, we found no proof to substantiate a MWP, but our data does confirm the occurrence of a pronounced dry period between ~ 1000 and 1200 A.D.

4.3.3 The Little Ice Age

The term Little Ice Age (LIA) describes a time period between the mid-16th century and 1850 with cooler conditions, expanded glaciation, and significantly altered climate conditions in and around Europe (Mann 2002). Both spatial extend and causes for the LIA are not clear. However, it is hypothesized that decreased solar activity (Bard & Frank 2006), decreased Earth's obliquity (Marcott et al. 2013) and increased freshwater discharge into the North Atlantic Ocean, as during the Younger Dryas discussed by Broecker et al. (1989) and later Condron and Winsor (2012), must have contributed to a LIA. But, since the LIA predominately occurred in and around Europe, the global signal of a LIA should hence be considered a time of modest cooling in the northern hemisphere (Mann 2002).

The temperature reconstructions indicate ~ 1.7°C lower temperatures than the 1901 to 2000 reference period with no considerable precipitation deviations. Simulated runoff shows continuous low streamflow. Simulated drought indices show no precipitation deficit and hence do not consider the LIA a dry period; the drought index by Kress et al. (2014) however does. The glacier mass balance is predominately positive indicating major glacier advances. On a decadal scale, the model detects the occurrence of the LIA being in coherency with other proxy records.

4.3.4 20th Century Warming

The 20th century is most likely the warmest of the millennium (Mann et al. 1999). Since 1970, more solar energy has been entering the Earth's atmosphere than exiting caused by increased greenhouse gas emissions (IPCC 2013) with a more pronounced winter than summer warming (Casty et al. 2005). While upward and downward trends are observed during the last century, climate variability can be contributed to varying aerosol emissions including volcanic eruptions, more pronounced to increased greenhouse gas emissions since the 1970s (IPCC 2013), an 11-year cycle of solar activity fluctuations (Bard & Frank 2006). However, as it is acknowledged that climate change is occurring and the last century is probably the warmest of the last two millennia, uncertainties remain on how the climate will influence Earth system processes in the future.

The temperature reconstructions indicate ~ 0.03°C lower temperatures than the 1901 to 2000 reference period, but ~ 0.6°C higher temperatures since the 1970's with no considerable precipitation deviations. In May 1999 and in August 2005, sustained rainfalls caused major flooding events in northern parts of Switzerland resulting in peak river and peak lake water levels (FOEN 2008). Simulated runoff indicates changes in runoff, but simulated peak runoff and peak precipitation values are assigned to 1997 rather than 1999, and in 2005 no noteworthy runoff anomaly is detected for the annually resolved datasets. For the monthly resolved datasets, peak runoff in May is detected without exceeding a critical threshold and in 2005 no considerable runoff is detected. Crucial processes resulting in floods are usually long lasting rainfall episodes followed by short heavy rainfalls causing floods on daily timescales (Frei 2006) making it nearly impossible to detect flooding events on monthly or annual timescales. Because an internal model error, the magnitudes of simulated total runoff cannot be considered, but the timing of the events however can. The glacier mass balance shows continuous negative mass balances except for a positive excursion during the late 1970s and 1980s. It has been observed that in the northern hemisphere mean annual air temperatures were decreased with an opposite trend in the southern hemisphere (Peterson et al. 2008) explaining this positive excursion. Also, when analyzing the observed Scaletta glacier data from the Swiss Glacier Network VAW/ETHZ & EKK/SCNAT, a noticeable advance is detectable around 1979 being in coherency with the model even though the statistical

results were statistically insignificant. This fact ultimately supports the hypothesis that regional trends are nevertheless detectable.

5. Conclusion

The first attempt to model hydrological cycles implementing tree-ring based climate reconstructions into the semi-distributed conceptual model PREVAH shows insignificant results. Correlation coefficients outside the calibration period of 1984 to 2012 indicate poor model performance. However, during the calibration period the model performs well. PREVAHs model configuration is highly idealistic thus HRUs are classified based on land use and soil type information from the calibration period of 1971 to 2012. It is very unlikely that both land use and soil type stayed the same over 1250 let alone 2500 years. If historical documentation on land use or pedogenetic information on soil type changes were available, it would still stay idealistic, because the parameterization procedure would most likely be based on subjective criteria rather than empirical relationships. Also, the information on sunshine duration, cloud cover, relative humidity and wind speed were randomly distributed 21 times based on the data from the calibration period from 1971 to 2012 biasing the results. However, because of an internal model error absolute values were computed falsely limiting any statistical analysis. Therefore it is unfair to judge the models performance outside the calibration period regarding randomly distributed pre-settings.

Regarding the tree-ring series, reconstructing an annual climate signal based on tree-ring chronologies is hardly possible. Any climate reconstruction will always be partially limited by the growing season and hence the term “seasonal reconstruction” is more appropriate. Also, the reconstructed precipitation should rather be treated as plant available water from precipitation and soil storage during the growing period other than as total seasonal precipitation. Since the precipitation reconstructions are poor, any attempt to model annually and monthly resolved hydrological cycles with poor precipitation estimates will end up with poor results, thus precipitation is the main input of water within a catchment water balance (Davie 2008). Both precipitation and temperature reconstructions were compiled over a broad spatial scale covering the Greater Alpine Region. The hydrological modelling system was applied for two spatially confined catchments in Switzerland. Even if annually temperature variations are rather homogenous for the Greater Alpine Region, precipitation variations are not. Switzerland lies near the right exit zone of the

southwest-northeast rotating polar front jet over the North Atlantic Ocean, between the Azores high pressure cell and the Icelandic low pressure cell. Orographic precipitation, strong downslope winds in the Alps and thermotopographical circulation systems make Swiss precipitation patterns, especially in the Alps, highly heterogeneous (Wanner et al. 1997). The negligence of heterogeneous precipitation patterns, even between the two catchments, is one crucial aspect why the models performance is questionable. Statistical improvements may be achieved if site specific tree-ring chronologies could be obtained from both the Murg and the Dischmabach catchments. However, it is generally difficult to reconstruct precipitation by its full extend using tree-ring estimates especially from tree sampling sites where precipitation is not the limiting factor.

When upscaling the temporal resolution and neglecting absolute values, PREVAH does detect paleohydroclimatic trends. The Roman Climate Optimum, the Little Ice Age and the 20th century warming are detected and the models results are in coherency with other proxy records. We found no proof to substantiate a MWP, but our data does confirm the occurrence of a pronounced dry period between ~ 1000 and 1200 A.D. The modelled paleohydroclimatic trends are however influenced by the tree-ring series and the detection of any paleohydroclimatic trend is highly tree-ring data dependent. Subsequently, trends are modelled if the tree-ring data show trends highlighting the importance of tree-ring data showing similarities with local climate anomalies (on catchment scales).

Last but not least, PREVAH remains a conceptual model and no matter how well the input parameters are, the output will always stay a simplification of reality.

6. Outlook

In order to successfully validate the models performance using tree-ring based climate reconstructions, the internal error needs to be identified and fixed. A subsequent repetition using the same model set-up would allow proper statistical analyses regarding absolute values. Numerous test statistics as suggest by Moriasi et al. (2007) could be conducted such as the Nash-Sutcliffe efficiency (Nash & Sutcliffe 1970), the percent bias (Gupta et al. 1999), mean square error, root mean square error, mean absolute error, the index of agreement (Legates & McCabe 1999) and the root mean square error-observations standard deviation ratio (Moriasi et al. 2007). If the results show statistically significant results, the model would extend the temporal resolution of the hydrological cycle extending the comprehension of physical, chemical and biological processes linked to natural hazards, extreme events, hydropower and water resource management (Viviroli et al. 2012). Further, the model could be optimized regarding tuneable parameterization procedures and the execution of trend analyses or extreme value statistics to evaluate return periods (i.e. Yue et al. 2002; Davie 2008) would also contribute to better future climate scenarios and interactions (i.e. Birsan et al. 2005; Lenderink et al. 2007).

It is an ongoing challenge in dendrochronology to increase the statistical significance reconstructing climate signals, especially for precipitation. While few scientists have achieved good statistical results reconstructing seasonal precipitation patterns with correlation coefficients as high as 0.69 (i.e. Akkemik et al. 2005), they still remain seasonal reconstructions. In order to model past hydrological cycles on an annual or even a monthly time scale, other proxy records could be considered in addition to tree-ring series to compliment the resolution. Noise could also be added to the tree-ring series to enhance the signals resolution using statistical techniques as suggested by Salas et al. (2014). Either way, since precipitation is the main input of water within a catchment water balance (Davie 2008), increasing the accuracy and the temporal resolution of proxy-based precipitation reconstructions may be of greater importance than improving an already existing hydrological model.

Tree-ring series with precipitation and temperature reconstructions were provided by Dr. Ulf Buentgen. Amongst other dendrochronologists he compiled tree-ring series

within the Greater Alpine Region over the last 1250 years and 2500 years, respectively. In this first attempt, we used two Swiss catchments with local climate variability. The tree-ring series might deflect broader scale climate trends, but do not represent local climate variability. Subsequently, either local tree-ring chronologies should be established within the model-catchments, or the hydrological model could be calibrated for a catchment near the tree-ring sampling sites to evaluate any spatial errors.

Last but not least, an overall comparison between modelling total runoff and reconstructing streamflow events using tree-ring data could provide basic information on which approach is more promising and where other potential errors are occurring.

Acknowledgments

I want to thank my supervisors Paolo, Massimiliano and Ulf for their support and their great effort to include me into their research units at the WSL. It was of great pleasure working at the WSL and I learned a lot. I also want to thank Markus for his support and for being a branch between the WSL and the Department of Geography at the University of Zurich. Additionally, I want to thank Ulf for providing tree-ring series and Dr. Anne Kress for providing her drought reconstructions. I also want to thank everybody in the Dendroecology and Dendroclimatology group at the WSL for treating me as a scientific member and for making my stay an absolute pleasure. Last but not least I want to thank my parents for supporting me morally and financially during my studies. I finally made it!

Thank you.

References

Literature

Akkemik, Ü.; Dağdeviren, N. & Aras, A. (2005): A preliminary reconstruction (A.D. 1635-2000) of spring precipitation using oak tree rings in the western Black Sea region of Turkey. International Journal of Biometeorology **49**: 297-302.

Akkemik, Ü; D'Arrigo, R.; Cherubini, P.; Koese, N. & Jacoby, G. C. (2008): Tree-ring reconstructions of precipitation and streamflow for north-western turkey. International Journal of Climatology **28**: 173-183.

Anderegg, W. R. L.; Berry, J. A.; Smith, D. D.; Sperry, J. S.; Anderegg, L. D. L. & Field, C. B. (2012): The roles of hydraulic and carbon stress in a widespread climate-induces forest die-off. Proceedings of the National Academy of Sciences of the United States of America **109**(1): 233-237.

Andréasson, J.; Bergström, S.; Carlsson, B.; Graham, L. P. & Lindström, G. (2004): Hydrological change – climate change impact simulations for Sweden. A Journal of the Human Environment **33**(4): 228-234.

Auer, I.; Boehm, R.; Jurkovic, A.; Lipa, W.; Orlik, A.; Potzmann, R.; Schoener, W.; Ungersboeck, M.; Matulla, C.; Briffa, K.; Jones, P.; Efthymiadis, D.; Brunetti, M.; Nanni, T.; Maugeri, M.; Mercalli, L.; Mestre, O.; Moisselin, J.-M.; Begert, M.; Mueller-Westermeier, G.; Kveton, V.; Bochnicek, O.; Statsny, P.; Lapin, M.; Szalai, S.; Szentimrey, T.; Cegnar, T.; Dolinar, M.; Gajic-Capka, M.; Zaninovic, K.; Majstorovic, Z. & Nieplova, E. (2007): HISTALP – historical instrumental climatological surface time series of the Greater Alpine Region. International Journal of Climatology **27**: 17-46.

Bard, E. & Frank, M. (2006): Climate change and solar variability: What's new under the sun? Earth and Planetary Science Letters **248**: 1-14.

Begert, M.; Schlegel, T. & Kirchhofer, W. (2005): Homogeneous temperature and precipitation series of Switzerland from 1864 to 2000. International Journal of Climatology **25**: 65-80.

Benn, D. I. & Lehmkuhl, F. (2000): Mass balance and equilibrium-line altitudes of glaciers in high-mountain environments. Quaternary International **65/66**: 15-29.

Bergström, S. & Singh, V. P. (1995): The HBV model. Computer Models of Watershed Hydrology: 443-476.

Birsan, M.-V.; Molnar, P.; Burlando, P. & Pfaundler, M. (2005): Streamflow trends in Switzerland. Journal of Hydrology **314**: 312-329.

Brázdil, R. & Kundzewicz, Z. W. (2006): Historical hydrology - Editorial. Hydrological Sciences Journal **51**(5): 733-738.

Brito-Castillo, L.; Díaz-Castro, S.; Salinas-Zavala, C. A. & Doulgas, A. V. (2003): Reconstruction of long-term winter streamflow in the Gulf of California continentl watershed. Journal of Hydrology **278**: 39-50.

Broecker, W. S. (2001): Was the Medieval Warm Period global? Science **291**(5508): 1497-1499.

Broecker, W. S.; Kennett, J. P.; Flower, B. P.; Teller, J. T.; Trumbore, S.; Bonani, G. & Wolfli, W. (1989): Routing of meltwater from the Laurentide Ice Sheet during the Younger Dryas cold episode. Nature **341**: 318-321.

Buentgen, U. & Tegel, W. (2011): European tree-ring data and the Medieval Climate Anomaly. Pages news **19**(1): 14-15.

Buentgen, U.; Frank, D. C.; Nievergelt, D. & Esper, J. (2006): Summer temperature variations in the European Alps, A.D. 755-2004. Journal of Climate **19**: 5606-5623.

Buentgen, U; Tegel, W.; Nicolussi, K.; McCormick, M.; Frank, D.; Trouet, V.; Kaplan, J. O.; Herzig, F.; Heussner, K.-U.; Wanner, H.; Luterbacher, J. & Esper, J. (2011): 2500 years of European climate variability and human susceptibility. Science **331**(6017): 578-582.

Bunn, A. G.; Sharac, T. J. & Graumlich, L. J. (2004): Using a simulation model to compare methods of tree-ring detrending and to investigate the detectability of low-frequency signals. Tree-Ring Research **60**(2): 77-90.

Casty, C.; Wanner, H.; Luterbacher, J., Esper, J. & Boehm, R. (2005): Temperature and precipitation variability in the European Alps since 1500. International Journal of Climatology **25**: 1855-1880.

Chiras, D. D. (2013): Environmental Science. Burlington, Massachusetts. Jones & Bartlett Learning: p. 73-95.

Condron, A. & Winsor, P. (2012): Meltwater routing and the Younger Dryas. Proceedings of the National Academy of Sciences of the United States of America **109**(49): 19928-19933.

Cook, E. R. & Jacoby, G. C. (1983): Potomac River streamflow since 1730 as reconstructed by tree rings. Journal of Climate and Applied Meteorology **22**(10): 1659-1672.

Cook, E. R.; Palmer, J. G. & D'Arrigo, R. D. (2002): Evidence for a 'Medieval Warm Period' in a 1,100 year tree-ring reconstruction of past austral summer temperatures in New Zealand. Geophysical Research Letters **29**(14): 12-1 – 12-4.

Copenheaver, C. A.; Gaertner, H.; Schaefer, I.; Vaccari, F. P. & Cherubini, P. (2010): Drought-triggered false ring formation in a Mediterranean shrubs. Botany **88**: 545-555.

Davie, T. (2008): Fundamentals of hydrology. Abingdon, Oxon. Routledge: p. 14-35; p. 101-124.

Dracup, J. A.; Lee, K. S. & Paulson, E. G. (1980): On the definition of droughts. Water Resource Research **16**(2):297-302.

Esper, J.; Wilson, R. J. S.; Frank, D. C.; Moberg, A.; Wanner, H. & Luterbacher, J. (2005): Climate: Past ranges and future changes. Quaternary Science Reviews **24**(20-21): 2164-2166.

Frei, C. (2006): Eine Länder übergreifende Niederschlagsanalyse zum August Hochwasser 2005. Ergänzung zu Arbeitsbericht 211. Arbeitsberichte der MeteoSchweiz **213**: 1-10.

Fritts, H. C. (1976): Tree rings and climate. Caldwell, New Jersey. Blackburn Press: p. 10-28; p. 412-433.

Graham, L. P.; Hagemann, S.; Jaun, S. & Beniston, M. (2007): On interpreting hydrological change from regional climate models. Climate Change **81**: 97-122.

Griggs, C.; DeGaetano, A.; Kuniholm, P. & Newton, M. (2007): A regional high-frequency reconstruction of May-June precipitation in the north Aegean from oak tree rings, A.D. 1089-1989. International Journal of Climatology **27**: 1075-1089.

Gupta, H. V.; Sorooshian, S.; Yapo, P.O. (1999): Status of automatic calibration for hydrologic models: Comparison with multilevel expert calibration. Journal of Hydrological Engineering **4**(2): 135-143.

Gurtz, J.; Baltensweiler, A. & Lang, H. (1999): Spatially distributed hydrotope-based modelling of evapotranspiration and runoff in mountainous basins. Hydrological Processes **13**: 2751-2768.

Hass, H. C. (1996): Northern Europe climate variations during late Holocene: Evidence from marine Skagerrak. Paleogeography, Paleoclimatology, Paleoecology **123**: 121-145.

Hay, L. E.; Wilby, R. L.; Leavesley G. H. (2000): A comparison of delta change and downscaled GCM scenarios for three mountainous basins in the United States. Journal of the American Water Resource Association **36**(2): 387-397.

Helama, S.; Lindholm, M.; Timonen, M. & Eronen, M. (2004): Detection of climate signal in dendrochronological data analysis: A comparison of tree-ring standardization methods. Theoretical and Applied Climatology **79**: 239-254.

Hoelzle, M.; Chinn, T.; Stumm, D.; Paul, F.; Zemp, M. & Haeberli, W. (2007): The application of glacier inventory data for estimating past climate change effect on mountain glaciers: A comparison between the European Alps and the Southern Alps of New Zealand. Global and Planetary Change **56**: 69-82.

Holmes, R. L.; Stockton, C. W. & LaMarche, V. C. (1979): Extension of river flow records in Argentina from long tree-ring chronologies. Water Resource Bulletin **15**(4): 1081-1085.

Holzhauser, H.; Magny, M. & Zumbuehl, H. J. (2004): Glacier and lake-level variations in west-central Europe over the last 3500 years. The Holocene **15**(6): 789-801.

Hughes, M. K. & Diaz, H. F. (1994): Was there a 'medieval warm period', and if so, where and when? Climate Change **26**(2-3): 1009-142.

Intergovernmental Panel on Climate Change IPCC (2013): The Physical Science Basis. Working group I contribution to the fifth assessment report of the Intergovernmental Panel on Climate Change. Cambridge. Cambridge University Press: p. 37-52.

Kress, A. (2009): Stable isotope dendroclimatology in the Swiss Alps: A 1200 - year record from European larch. Doctoral dissertation. Swiss Federal Institute of Technology ETH, Zurich. Diss. ETH No. 18535: p. 75-130.

Kress, A.; Hangartner, S.; Bugmann, H.; Buentgen, U.; Frank, D. C.; Leuenberger, M.; Siegwolf, R. T. W. & Saurer M. (2014): Swiss tree rings reveal warm and wet summers during medieval times. Geophysical Research Letters **41**: 1732-1737.

LaMarche, V. C. (1978): Tree-ring evidence of past climatic variability. Nature **276**: 334-338.

Lamb, H. H. (1965): The early medieval warm period epoch and its sequel. Paleogeography, Paleoclimatology, Paleoecology **1**: 13-37.

Legates, D. R. & McCabe, G. J. (1999): Evaluating the use of "goodness-of-fit" measures in hydrologic and hydroclimatic model validation. Water Resource Research **35**(1): 233-241.

Lenderink, G.; Buishand, A. & Van Deursen, W. (2007): Estimates of future discharges of the river Rhine using two scenario methodologies: Direct versus delta approach. Hydrology & Earth System Sciences **11**(3): 1145-1159.

Lindström, G.; Johansson, B.; Persson, M.; Gardelin, M. & Bergström, S. (1997): Development and test of the distribution HBV-96 hydrological model. Journal of Hydrology **201**: 272-288.

Mann, M. E. (2002): Little ice age. Encyclopedia of global environmental change **1**: 504-509.

Mann, M. E.; Bradley, R. S. & Hughes, M. K. (1999): Northern hemisphere temperatures during the past millennium: Inferences, uncertainties, and limitations. Geophysical Research Letters **26**(6): 759-762.

Marcott, S. A.; Shakun, J. D.; Clark, P. U. & Mixm A. C. (2013): A reconstruction of regional and global temperature for the past 11,300 Years. Science **339**(6124): 1198-1201.

McDowell, N. (2011): Mechanisms linking drought, hydraulics, carbon metabolism, and vegetation mortality. Plant Physiology **155**: 1051-1059.

McDowell, N.; Pockman, W. T.; Allen, C. D.; Breshears, D. D.; Cobb, N.; Kolb, T.; Plaut, J.; Sperry, J.; West, A.; Williams, D.G. & Yepez, E.A. (2008): Mechanisms of plant survival and mortality during drought: Why do some plants survive while others succumb to drought? New Phytologist **178**: 719-739.

Moriasi, D. N.; Arnold, J. G.; Van Liew, M. W.; Bingner, R. L., Harmel, R. D. &Veith, T. L. (2007): Model evaluation guidelines for systematic quantification of accuracy in watershed simulations. Transactions of the American Society of Agricultural and Biological Engineers **50**(3): 885-900.

Nash, J. E. & Sutcliffe, J. V. (1970): River flow forecasting through conceptual models: Part 1. A discussion of principles. Journal of Hydrology **10**(3): 282-290.

Peterson, T. C.; Connolley, W. M. & Fleck, J. (2008): The myth of the 1970s global cooling scientific consensus. Bulletin of the American Meteorological Society **89**(9): 1325-1337.

Raper, S. C. B. & Braithwaite, R. J. (2009): Glacier volume response time and its links to climate topography based on a conceptual model of glacier hypsometry. The Cryosphere **3**: 183-194.

Reale, O. & Dirmeyer, P. (2000): Modeling the effects of vegetation on Mediterranean climate during the Roman Classical Period part I: Climate history and model sensitivity. Global and Planetary Change **25**(3-4): 163-184.

Sala, A. (2009): Lack of direct evidence for the carbon-starvation hypothesis to explain drought-induced mortality in trees. Proceedings of the National Academy of Sciences of the United States of America, **106**(26): E68.

Salas, J. D.; Tarawneh, Z. & Biondi, F. (2014): A hydrological record extension model for reconstructing streamflows from tree-ring chronologies. Hydrological Processes.

Schaer, C.; Vidale, P. L.; Luethi, D.; Frei, C.; Haeberli, C.; Liniger, M. A. & Appenzeller, C. (2004): The role of increasing temperature variability in European summer heatwaves. Nature **427**(6972): 332-336.

Seibert, J. (1997): Estimation of parameter uncertainty in the HBV model. Nordic Hydrology **28**(4/5): 247-262.

Stanley, S. M. (2009): Erath System History. New York, New York. W. H. Freeman and Company: p. 495-520.

Swiss Federal Office for the Environment FOEN (2008): Hochwasser 2005 in der Schweiz. Synthesebericht zur Ereignisanalyse. www.umwelt-schweiz.ch/div-7529-d.

Thornthwaite, C. W. (1948): An approach toward a rational classification of climate. Geographical Review **38**(1): 55-94.

Viviroli, D.; Zappa, M.; Gurtz, J. & Weingartner, R. (2009): An introduction to the hydrological modelling system PREVAH and its pre- and post-processing-tools. Environmental Modelling & Software **24**: 1209-1222.

Wallis, J. R. & O'Connell, P. E. (1973): Firm reservoir yield – how reliable are historic hydrological records? Hydrological Science Bulletin **18**(3): 147-365.

Wanner, H.; Rickli, R.; Salvisberg, E.; Schmutz, C. & Schüepp, M. (1997): Global climate change and variability and its influence on Alpine Climate – Concepts and Observations. Theoretical and Applied Climatology **58**: 221-243.

Wilhite, D. A. & Glantz, M. H. (1985): Understanding the Drought phenomenon: The role of definitions. Water International **10**(3): 111–120.

Yue, S.; Pilon, P. & Cavadias, G. (2002): Power of the Mann-Kendall and Spearman's rho tests for detecting monotonic trends in hydrological series. Journal of Hydrology **259**: 254-271.

Zappa, M.; Bernhard, L.; Fundel, F. & Joerg-Hess, S. (2012): Vorhersage und Szenarien von Schnee- und Wasserressourcen im Alpenraum. Forum für Wissen: 19-27.

Climatological and Hydrological Data

Historical Instrumental Climatological Surface Time Series of the Greater Alpine Region HISTALP: Homogenized temperature and precipitation data from the Greater Alpine Region. http://www.zamg.ac.at/histalp (last access: February 10th 2014).

Swiss Federal Office for Meteorology and Climatology MeteoSwiss: Homogenized temperature and precipitation data from Basel-Binningen, Geneva-Cointrin, Bern-Zollikofen and Zurich. http://www.meteoschweiz.admin.ch/web (last access: February 4th 2014).

Swiss Federal Office for the Environment FOEN: Runoff data for the Murg and Dischmabach streams. http://www.hydrodaten.admin.ch/ (last access: June 25th 2014).

Swiss Glacier Network VAW/ETHZ & EKK/SCNAT: Length-change data for the Scaletta glacier and the Silvrettaglacier. http://glaciology.ethz.ch/messnetz/index.html (last access: August 26th 2014).

Appendix

1. Simulated Runoff

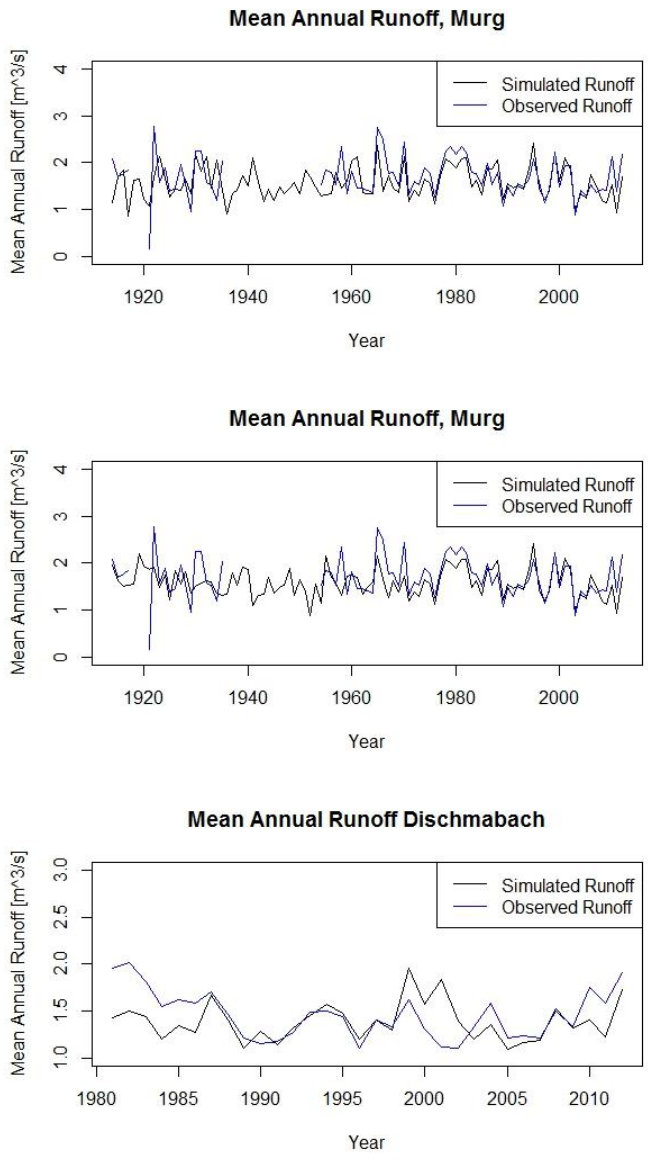

Figure 5: Simulated vs. observed runoff.

Top: Dendro 2500 for the Murg catchment. Middle: Dendro 1250 for the Murg catchment Bottom: Both Dendro-Files for the Dischmabach catchment.

Simulated annual runoff (black) is plotted with the observed annual runoff (blue) in figure 5, and as a time series displaying also the precipitation anomaly obtained by tree-ring chronologies in blue (figure 6). In figures 7 and 8, the monthly simulated runoff is plotted with the monthly observed runoff. Between 1918 and 1921 and between 1936 and 1953 no observed runoff data for the Murg catchment was available.

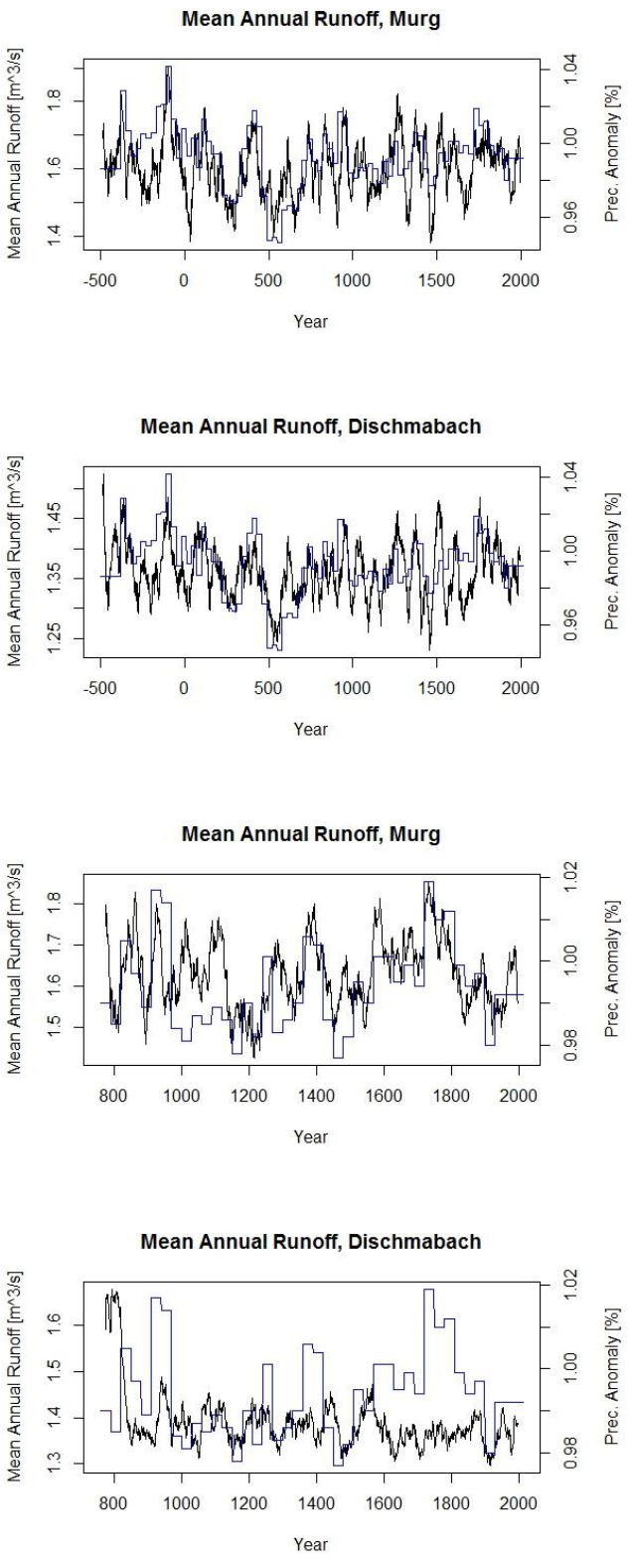

Figure 6: Simulated runoff (black) and precipitation anomalies (blue).

Top: Dendro 2500 for both the Murg and the Dischmabach catchment. Bottom: Dendro 1250 for both the Murg and the Dischmabach catchment.

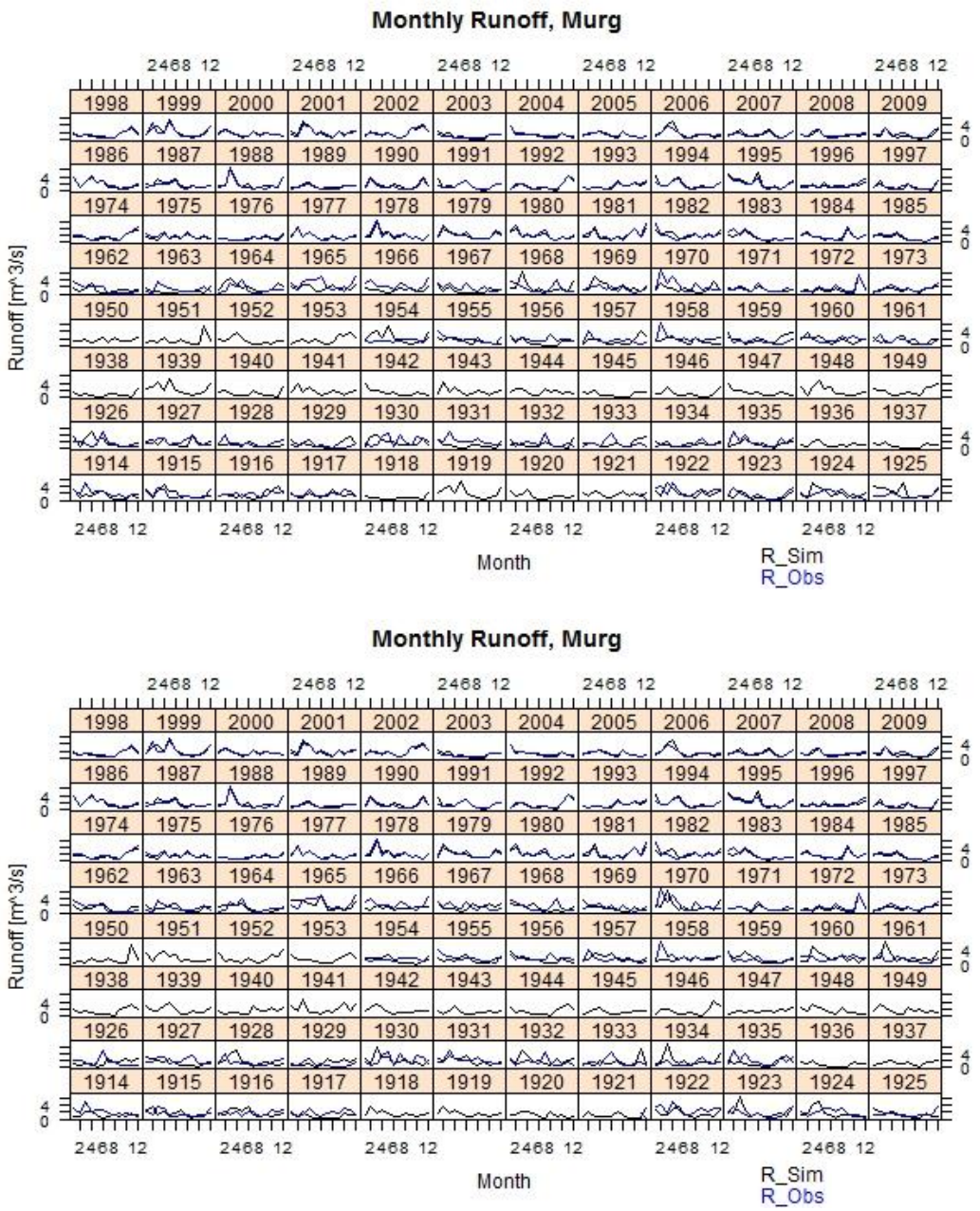

Figure 7: Simulated vs. observed monthly runoff, Murg.

Top: Dendro 2500. Bottom: Dendro 1250.

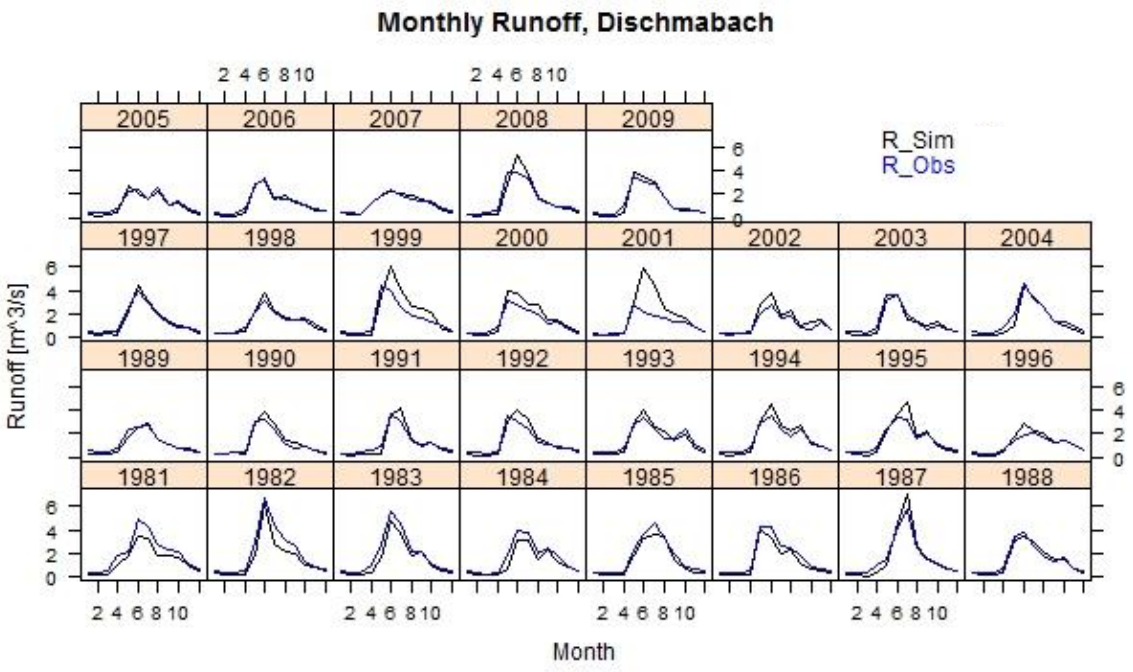

Figure 8: Simulated vs. observed monthly runoff, Dischmabach.

2. Mass Balance and Length Change Models for the Scaletta Glacier

The modelled mass balances for the Scaletta glacier are plotted in figures 11 and 12 applying a 50 year filter for visualization purposes. The modelled length change for the Scaletta glacier compared to observed length changes (Scaletta glacier and Silvrettaglacier) are shown in figures 13 and 14.

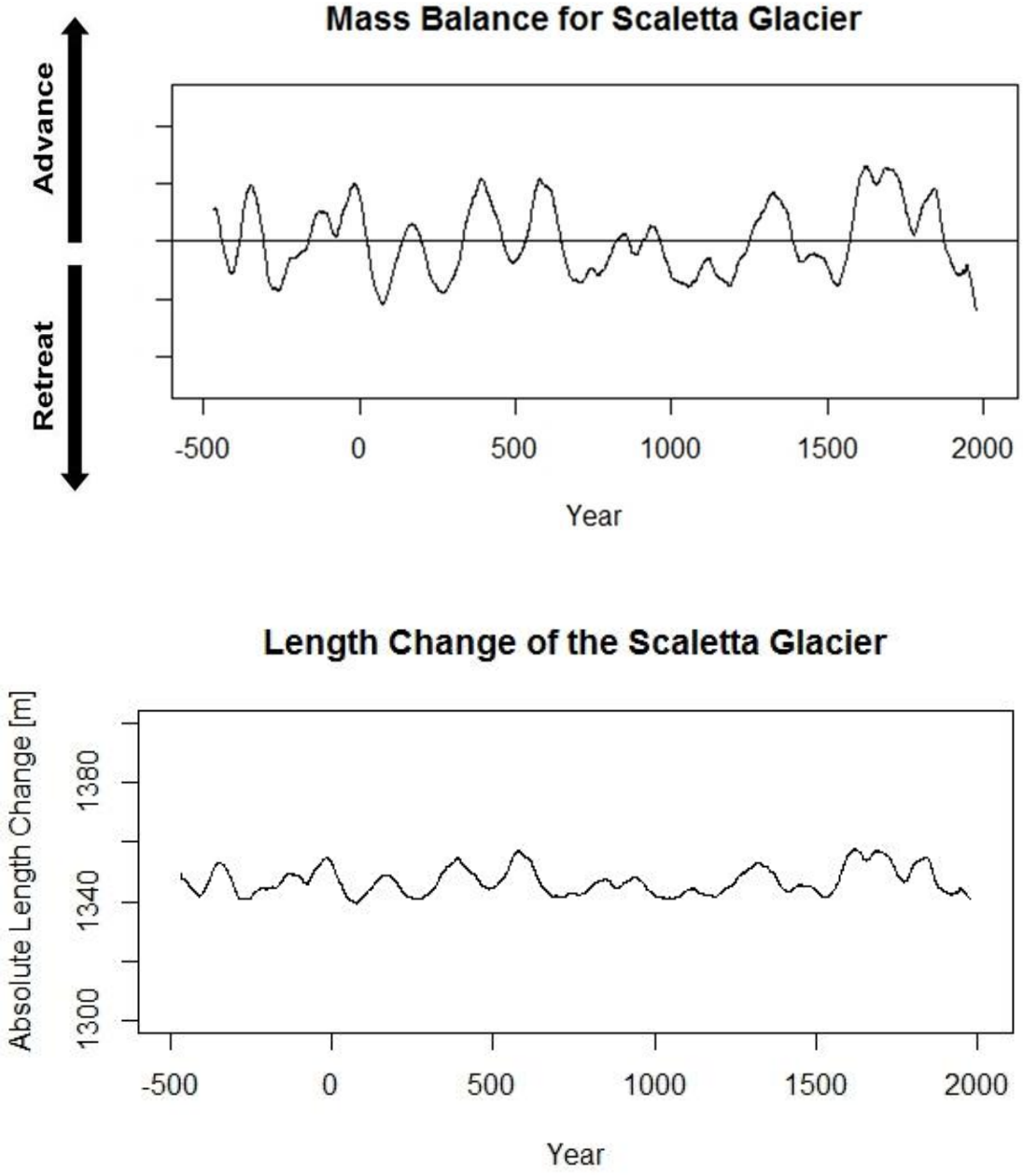

Figure 9: Modelled mass balance and length change for the Scaletta glacier.

File: Dendro 2500.

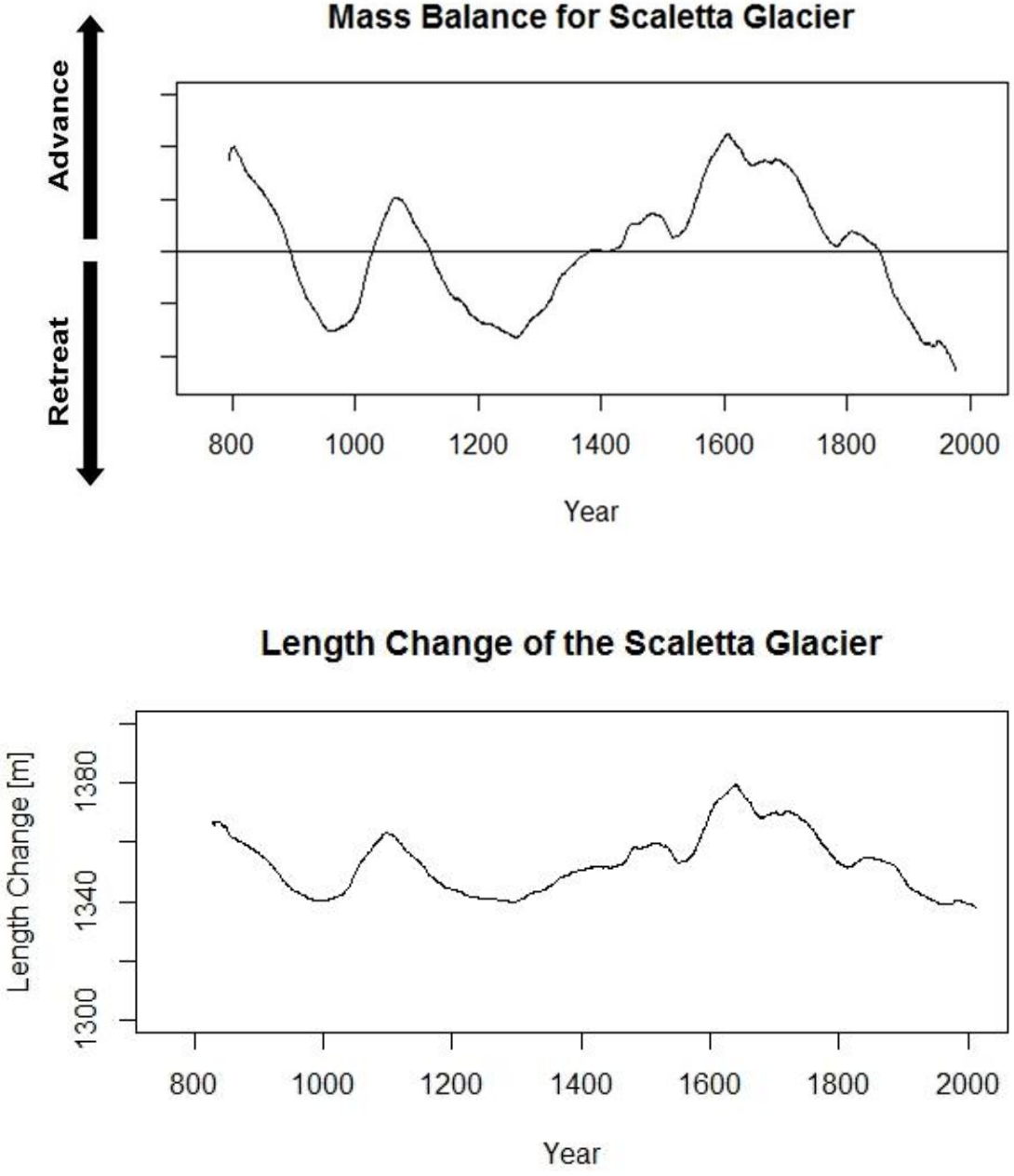

Figure 10: Modelled mass balance and length change for the Scaletta glacier.

File: Dendro 1250.

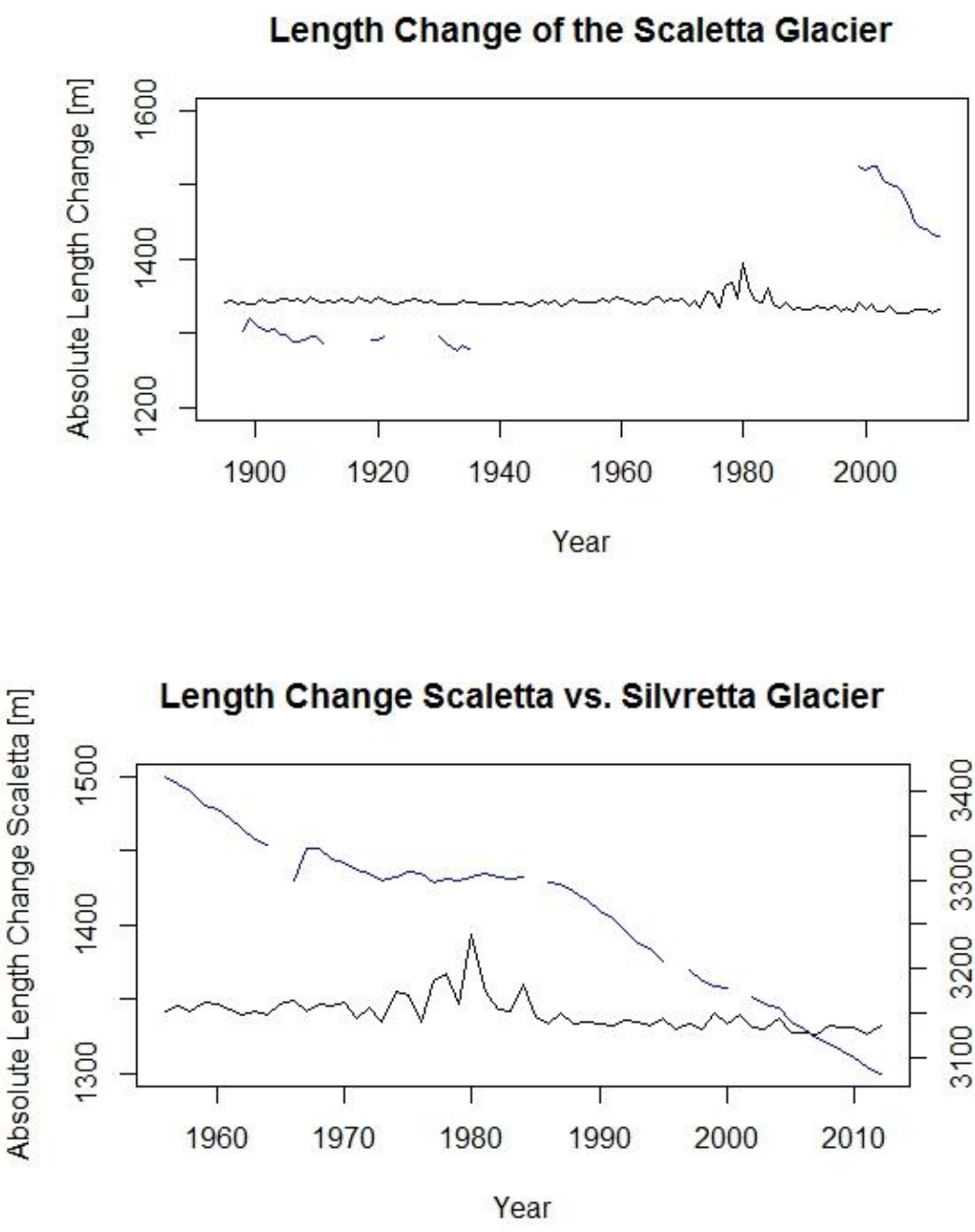

Figure 11: Modelled length change.

Top: Simulated (black) vs. observed (blue) length change for the Scaletta glacier. Bottom: Simulated length change for the Scaletta glacier (black) vs. observed length change for the Silvrettaglacier (blue).

File: Dendro 2500.

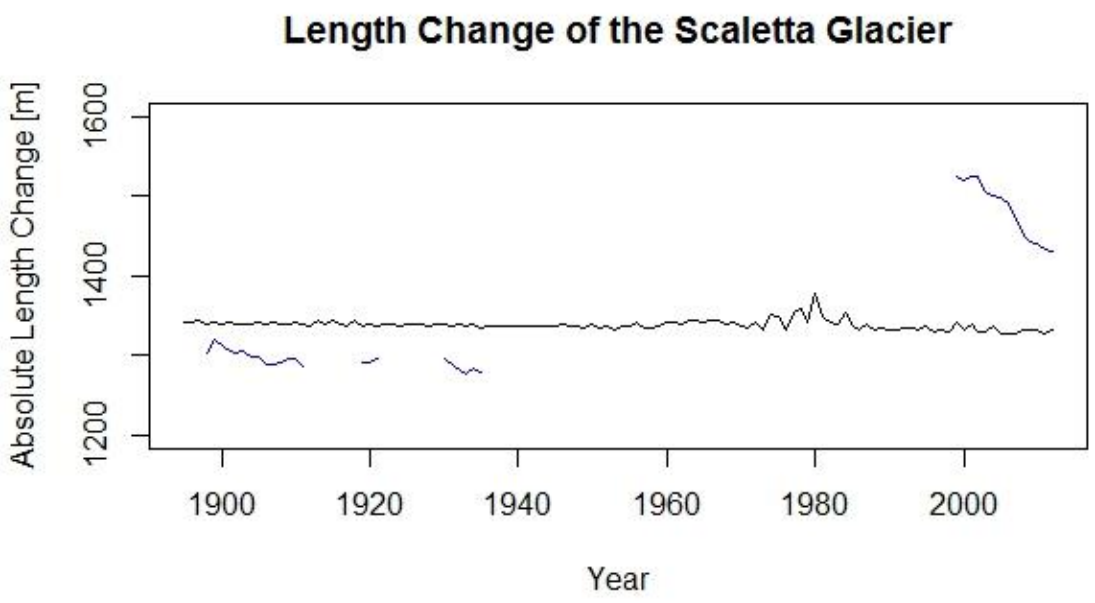

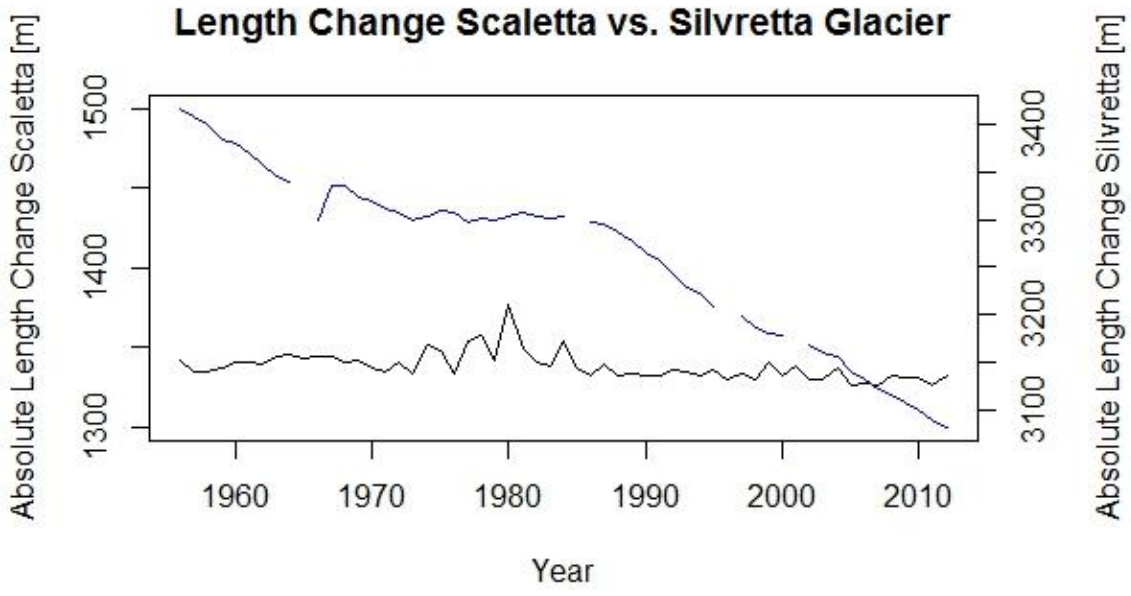

Figure 12: Modelled length change.

Top: Simulated (black) vs. observed (blue) length change for the Scaletta glacier. Bottom: Simulated length change for the Scaletta glacier (black) vs. observed length change for the Silvrettaglacier (blue).

File: Dendro 1250.

3. Drought Indices

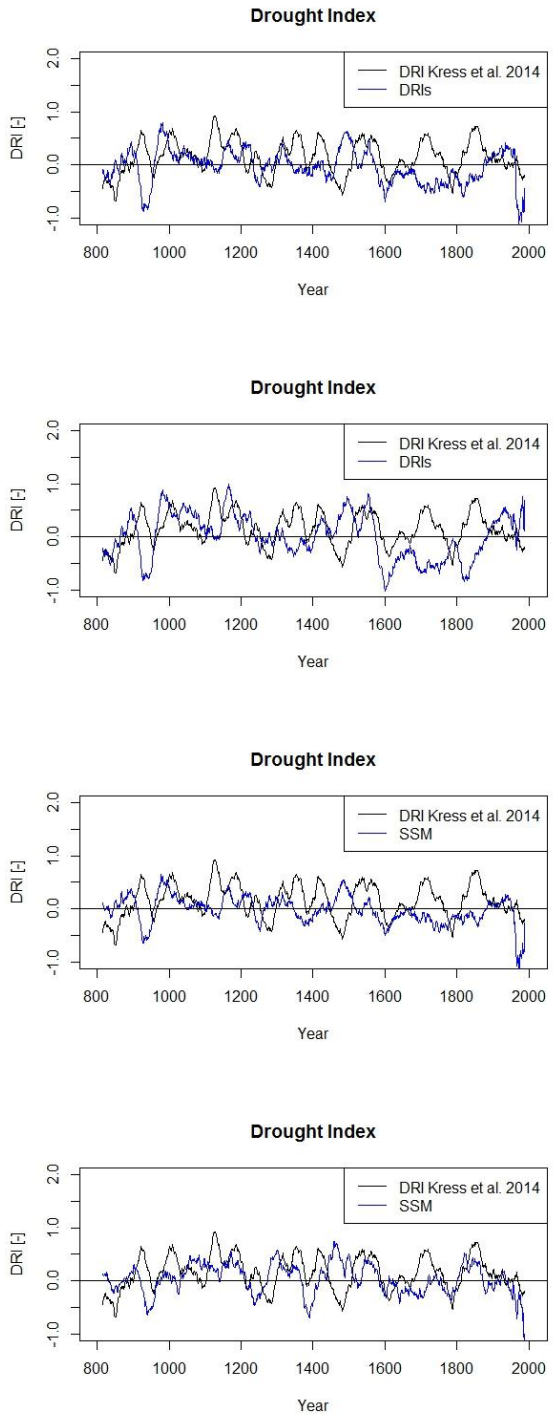

Figure 13: Drought indices.

Top: Dendro 2500 DRIs for both the Murg (upper) and the Dischmabach (lower) catchment. Bottom: Dendro 2500 SSM for both the Murg (upper) and the Dischmabach (lower) catchment.

The modelled drought indices (DRIs, SSM) were compared with the drought index from Kress et al. (2014).

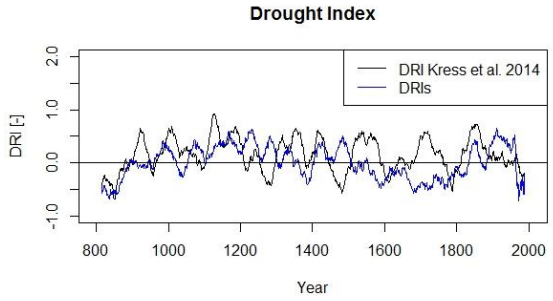

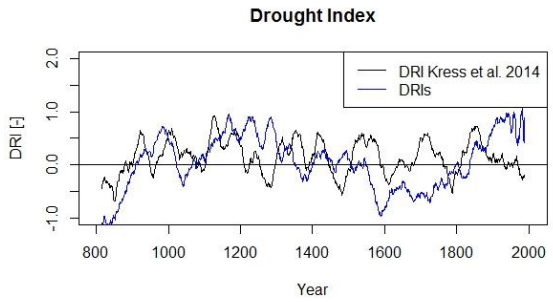

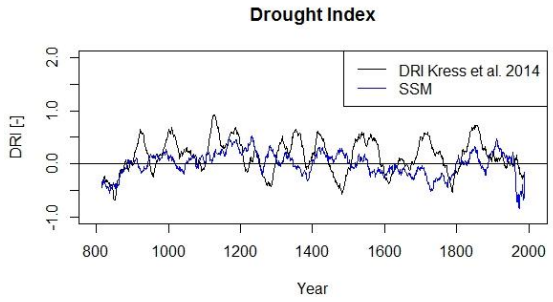

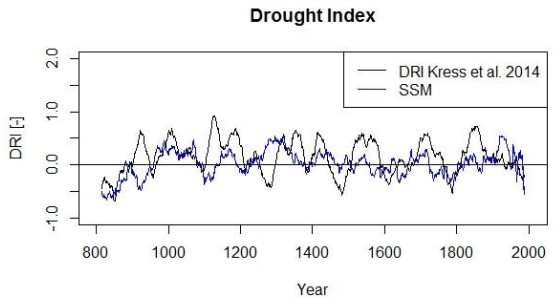

Figure 14: Drought indices.

Top: Dendro 1250 DRIs for both the Murg (upper) and the Dischmabach (lower) catchment. Bottom: Dendro 1250 SSM for both the Murg (upper) and the Dischmabach (lower) catchment.

Personal Declaration

I hereby declare that the submitted thesis is the result of my own, independent work. All external sources are explicitly acknowledged in the thesis.

Zurich, September 29th 2014

Eric Gasser